AAEC/E579

AAEC/E579

AUSTRALIAN ATOMIC ENERGY COMMISSION

RESEARCH ESTABLISHMENT

LUCAS HEIGHTS RESEARCH LABORATORIES

INVESTIGATION OF THE RESPONSE OF A NEUTRON MOISTURE METER USING A MULTIGROUP, TWO-DIMENSIONAL DIFFUSION THEORY CODE

by

A.I.M. RITCHIE
D.J. WILSON

December 1984

ISBN 0 642 59797 9

AUSTRALIAN ATOMIC ENERGY COMMISSION
RESEARCH ESTABLISHMENT
LUCAS HEIGHTS RESEARCH LABORATORIES

INVESTIGATION OF THE RESPONSE OF A NEUTRON MOISTURE METER USING A MULTIGROUP, TWO-DIMENSIONAL DIFFUSION THEORY CODE

by

A.I.M. RITCHIE
D.J. WILSON

ABSTRACT

A multigroup diffusion code has been used to predict the count rate from a neutron moisture meter for a range of values of soil water content ω, thermal neutron absorption cross section S_a (defined as Σ_a/ρ) of the soil matrix and soil matrix density ρ that encompasses most of the practical range of interest. Two dimensions adequately approximated the geometry of the source, detector and soil surrounding the detector. Seven energy groups, the data for which were condensed from 128 group data set over the neutron energy spectrum appropriate to the soil-water mixture under study, proved adequate to describe neutron slowing-down and diffusion. The soil-water mixture was an SiO_2-water mixture, with the absorption cross section of SiO_2 increased to cover the range of Σ_a required. The size of the system was chosen large enough to be effectively infinite at the lowest values of ω, S_a and ρ.

The effect of resonance capture was investigated by adding a group in the resonance energy range, with capture data appropriate to 1/v and non-1/v capture. The effect of any variation in scattering cross section of the matrix S_s (defined as Σ_s/ρ) was investigated by adding varying amounts of carbon to the soil-water mixture.

Ignoring the effect of resonance capture leads to errors in estimates of the soil-water content of up to a few per cent but only at concentrations of resonant absorbers which could be inferred from the mineralisation of the region or from the high S_a of the soil. Changes of about 5 per cent in S_s can produce changes of up to about 10 per cent in apparent water content.

The response to changes in matrix density is, in general, linear but the response to changes in water content is not linear over the range of parameter values investigated. Tabular results are presented which allow interpolation of the response for a particular ω, S_a and ρ. It is shown that $R(\omega, S_a, \rho) = \rho\, M(S_a) + C(\omega)$ is a crude representation of the response over a very limited range of variation of ω, and S_a. As the response is a slowly varying function of ρ, S_a and ω, a polynomial fit will provide a better estimate of the response for values of ρ, S_a and ω not tabulated.

National Library of Australia card number and ISBN 0 642 59797 9

The following descriptors have been selected from the INIS Thesaurus to describe the subject content of this report for information retrieval purposes. For further details please refer to IAEA-INIS-12 (INIS: Manual for Indexing) and IAEA-INIS-13 (INIS: Thesaurus) published in Vienna by the International Atomic Energy Agency.

COMPUTER CALCULATIONS; COMPUTER CODES; DENSITY; ERRORS; MOISTURE GAGES; NEUTRON FLUX; RESONANCE ABSORPTION; SCATTERING; SOILS; THERMAL NEUTRONS; WATER

CONTENTS

1. INTRODUCTION

The spatial dependence of the neutron flux about a point source of thermal neutrons in an infinitely large system is given by

$$\phi(r) = \frac{S}{4\pi D_t r} e^{-\kappa r} , \quad (1)$$

where $1/\kappa$ = the diffusion length,
D_t = the thermal neutron diffusion coefficient = $(3\Sigma_{tr})^{-1}$
Σ_{tr} = the macroscopic thermal neutron transport cross section.
S = source strength (neutrons s^{-1})
r = distance from the source.

If κr is small then the flux is approximated by

$$\phi(r) = \frac{3S}{4\pi r} \Sigma_{tr} , \quad (2)$$

and, if the medium surrounding the neutron source is soil with water density ω and matrix density ρ, equation 2 can be written as

$$\phi(r) = \frac{3S}{4\pi r} (\omega\Sigma_{tr}^{w} + \rho\Sigma_{tr}^{s}) \quad (3)$$

where Σ_{tr}^{w} and Σ_{tr}^{s} are the thermal neutron transport macroscopic cross section of water and soil respectively. The count rate in a thermal neutron detector at a distance r from the source then has a simple linear relationship with the water density in the soil. Moreover, since the thermal neutron macroscopic transport cross section of water ($\sim$ 2.33 cm^{-1}) is much larger than that of most soil constituents (e.g. 0.109 cm^{-1} for SiO_2 at a density of 1 g cm^{-3}), the count rate is approximately proportional to the water density.

This then is the basis of the design of neutron moisture meters that have been used for a number of years to determine the moisture levels in soils [Honig et al. 1971; Zuber and Cameron 1966] and in some other applications, for example the moisture levels in cereals [Ballard and Ely 1961]. The technique has the advantages that measurements can be done quickly and easily in the field, no great skill is required in operating the field equipment, and repeat measurements can be made at the same point in the soil over a period of time with no perturbation to the medium, apart from the initial introduction of the probe hole.

Unfortunately, since thermal neutron sources as such do not exist, a practical neutron moisture meter consists of a fast neutron ($\sim$ 1 MeV) source with an associated thermal neutron detector, the surrounding medium being used to slow the fast neutrons down to thermal energies. The simplest approach in this situation is to use age theory to describe neutron slowing down, and diffusion theory to describe the transport of the thermal neutrons. Such an approach [Jakeman 1966] predicts the thermal flux to be

$$\phi(r) = \frac{S}{8\pi D_t r} e^{\kappa^2\tau} \{e^{-\kappa r}[1-erf(\kappa\tau^{1/2}-r/2\tau^{1/2})] - e^{\kappa r}[1-erf(\kappa\tau^{1/2}+r/2\tau^{1/2})]\} \quad (4)$$

where τ = the age from the source energy E_o to thermal energies E_{th}

$$= \int_{E_{th}}^{E_o} \frac{D(E)}{\sum_i \xi_i \Sigma_i(E)} \frac{dE}{E}$$

where D(E) is the diffusion coefficient at energy E, and other quantities are defined in standard texts on neutron transport (see, for example, Weinberg and Wigner 1958). It is a reasonable approximation to take the scattering cross sections and the diffusion cross section D(E) as constant over the range $E_{th} \leq E \leq E_o$, and write

$$\tau = \frac{D}{\sum_i \xi_i \Sigma_i} \log(E_o/E_{th}) .$$

Even with this simplifying assumption, it is clear that the linear relationship that exists between the thermal flux and the water density in equation (3) is not apparent in equation (4).

Several authors [e.g. Gardner and Kirkham 1952; Holmes 1956; Andrieux et al. 1962; Semmler 1963] have used age theory methods. While this theory is very useful in providing a qualitative picture using

essentially hand calculations and good quantitative answers when the scattering medium is composed of heavy nuclei, it is not adequate to describe a system with a high hydrogen content where there are significant anisotropic scatter and energy exchange during the slowing down process. Olgaard [1965] has used three-group diffusion theory to improve on earlier age-theory calculations and achieved good agreement with some experimental measurements in various soil types. It is, however, surprising, in view of the many neutron transport codes and data sets available from the field of reactor physics, that, apart from some calculations appropriate to special geometries [Hearst 1968, 1974], there is little evidence in the open literature of more accurate calculations than those of Olgaard.

In this study, we have used a multigroup diffusion theory code to calculate the effect of such parameters as soil-water density, matrix density, matrix thermal absorption cross section and matrix scattering cross section on the thermal flux at a distance from a fast source, typical of the source-detector separation used in neutron moisture meters. We assume that the neutron moisture meter probe requires a neutron source and a neutron detector to be lowered down a 0.05 to 0.1 m borehole into soil or some other material, and do not consider moisture meters which are designed to measure near-surface moisture using a probe placed at the surface of the material. We have ignored the effect of self-absorption in the detector and neutron source, the effect of streaming in the probe hole and the effect of the thickness and material composition of the liner of the probe hole. Although all these will influence the detailed response of the neutron moisture meter, they are effects which cannot be adequately accounted for using a diffusion theory code. Moreover, with the geometries typical of neutron moisture meters under consideration it is reasonable to expect that these effects will not alter the neutron energy spectrum significantly in the region of the detector, but will appear rather as a scaling factor on the neutron flux. Such a factor will vanish when the count rate is considered relative to the count rate with the probe in a standard assembly, such as an infinitely large water system.

The effect of resonance absorption in the epithermal region on the thermal flux has also been studied. If such an effect is significant then we must find out whether or not there are strong resonance absorbers in the soil under study and the energies at which the resonances occur. This implies the need for detailed and expensive chemical analysis. If, however, only the thermal absorption cross section is of significance, the absorption can be characterised by a 1/v absorption term, with no need to know in detail the nuclei that contribute to the absorption.

2. CALCULATIONAL METHOD

2.1 Parameters and Their Range of Variation

The thermal flux in a thermal neutron detector placed some distance from a fast neutron source surrounded by a water-soil medium was taken to be a function of the following parameters:

(i) The total water density, ω in g cm^{-3}. This is the total water density, irrespective of whether the water is classified as free water, or as water bound in water of crystallation or in some other semi-chemical bond.

(ii) The matrix density, ρ, in g cm^{-3}, i.e. the density of material, other than water, that comprises the soil. In practice, it is the density of oven-dried soil less the density of bound water.

(iii) The thermal neutron mass absorption cross section of the soil matrix, defined as $S_a = \Sigma_a/\rho$, cm^2 g^{-1}, where Σ_a is the thermal neutron macroscopic absorption cross section. The absorption cross section is that for oven-dried soil corrected for the absorption cross section of bound water.

(iv) The mass scattering coefficient of the soil matrix $S_s = \Sigma_s/\rho$ cm^2 g^{-1}, where Σ_s is the macroscopic scattering cross section of the soil matrix. As with the absorption cross section this is the cross section for oven-dried soil corrected for any bound water content.

The total water density and matrix density were varied respectively from 0.1 to 0.4 g cm^{-3} and from 0.5 to 2.0 g cm^{-3}, ranges of considerable practical interest in soil and water measurements. The thermal mass absorption coefficient was varied from 1.70×10^{-3} cm^2 g^{-1}, the value for pure SiO_2, to 18.91×10^{-3} cm^2 g^{-1}, a range which covers the soils investigated by Graecan and Schrale [1976], Olgaard [1965] and our own investigations in mine overburden dumps [Daniel et al. 1980]. The matrix mass scattering coefficient was varied from 0.109 cm^2 g^{-1}, the cross section of SiO_2, to 0.13 cm^2 g^{-1}, again a range typical of the composition of many soils.

The mass absorption and scattering coefficients were used, rather than the more familiar macroscopic absorption and scattering cross sections, for two reasons: it is frequently easier to measure soil parameters per unit mass than per unit volume; manipulation of the scattering and absorption parameters to provide input data to the nuclear codes used for the various soil-water mixtures investigated was considerably simplified.

2.2 System Geometry

The source, probe and scattering medium were modelled in cylindrical geometry with the source and detector on the axis of the cylinder (see Figure 1). Such a geometry is a reasonable representation of the physical arrangement of most neutron moisture meters, in particular, those that use a Li-glass scintillator as the thermal neutron detector such as the one shown in Figure 2. The geometry also allows the source-detector separation to be treated as variable. In principle, such a representation also allows the detailed material composition of such items as the neutron source and the γ shield between the source and detector, and of the detector itself to be included, and their effects calculated. However, the large change in neutron mean free path in crossing the boundaries of these entities and the size of these entities which is small compared to the mean free paths, would provide a severe test of the diffusion theory used in the calculations. Any such calculation would need to be checked against other calculational tools, such as a transport theory code or a Monte Carlo code, or against experimental results.

In the present series of calculations, the thermal flux at the centre of the detector position was taken as a measure of the probe count rate and the source of neutrons assumed situated at the centre of the cylindrical volume delineating the actual neutron source volume. No specific account was taken of any perturbing effect of the detector or of the source material. Such effects will be considered in a later series of calculations.

Apart from the question of modelling the geometry of the system, there are the questions of how large the system must be to make it effectively infinite and what mesh interval to choose. The size is determined by the water density of the soil-water mixture - the greater the water density, the smaller the physical size need be to make the system appear infinite. To avoid continual changes in the size chosen for the system, calculations were done with water densities at 0.01 g cm $^{-3}$ to find the size where any increase in size produced less than 0.1 per cent changes in the thermal flux at the probe. This size, 300 cm long and 150 cm radius was used for all soil-water mixtures considered. Check calculations further showed that sufficient accuracy could be maintained using 29 radial and 76 axial mesh points.

2.3 Neutronics Codes Used

Ancillary to the problem of carrying out a multigroup diffusion calculation are the questions of choosing data appropriate to the nuclei present in the soil-water mixture and of producing mass coefficients that are averaged over the appropriate neutron energy spectrum. The AUS modular system [Robinson 1975] of nuclear reactor neutronics codes was used for this task. The library of the system contains cross section data, derived in the main from the ENDF/B library [Honek 1964], for a large number of nuclei in the form of cross sections averaged over 128 groups spanning the energy range 15 MeV to 1.318×10^{-3} eV. The MIRANDA code [Robinson 1977] of the AUS system was used in the bulk of the calculations to condense the 128 group cross sections for the nuclei taken to form a particular soil-water mixture, to a 7-group cross section set using a neutron energy spectrum appropriate to that soil-water mixture. Seven groups, whose boundaries are given in Table 1, were found sufficiently accurate over the range of soil-water mixtures covered.

POW [Pollard 1974], another module of the AUS system, is a three-dimensional multigroup diffusion theory code which, in the present case, was used to calculate the flux distribution in the two-dimensional representation of the system shown in Figure 1. In particular, the code was used to calculate the thermal flux at the detector position to investigate changes in the response of the probe as such parameters as water density and matrix density were varied.

To estimate the effects of resonance capture, an element with resonance capture was added to the soil-water mixture and a further energy group added to the 7-group set to accommodate the resonance region of the element. The non-1/v resonance absorption in this group was calculated using the code RESIN [Robinson 1980], which modified the resonance integral for the element at infinite dilution to account for both the concentration of resonance absorber in the soil-water mixture and the scattering properties of the soil-water mixture. A further calculation evaluated the appropriate group average mass coefficient for the soil-water-absorber mixture but with the assumption of 1/v behaviour for absorption in the resonance absorber over the whole energy range. The absorption cross section in the 'resonance' group of this latter

data set was then increased by the factor required to account for the total of 1/v and resonance absorption.

2.4 System Specification

Most systems studied were composed of mixtures of SiO_2 and water, the respective proportions being determined by the parameters ρ and ω. The cross sections of silicon, oxygen and water were combined by the code MIRANDA to give a cross section set for each mixture. It should be stressed that the cross sections in the thermal region for water were those appropriate to water and took proper account of the chemical bonding in the water molecule.

The thermal absorption cross section of the matrix was varied by multiplying the absorption cross section in the thermal group by a suitable factor. Except when the question of resonance absorption was being specifically examined, the mass absorption coefficient was assumed to have a 1/v dependence and hence the mass absorption coefficient in all other groups was scaled by the same factor as that of the thermal group. The thermal absorption coefficients quoted in this paper are the absorption coefficients for neutrons of velocity 2200 m s^{-1} and not in fact the average absorption coefficients for the 'thermal' group. These average values will change as the neutron energy spectrum changes with changes in the ratios of soil, water and absorber concentration.

The scattering coefficient was varied by adding differing amounts of carbon to the mixture. This was a simple thing to do using the MIRANDA data set and has the advantage that, since carbon has a very small mass absorption coefficient (1.7×10^{-4} cm^2 g^{-1}) but quite a large mass scattering coefficient (0.2725 cm^2 g^{-1}), compared to SiO_2 at 1.7×10^{-3} cm^2 g^{-1} and 0.109 cm^2 g^{-1} respectively, small additions of carbon change the scattering coefficient of the mixture significantly but alter the absorption coefficient by only a small amount. It also represents in a reasonable fashion, the variation in the scattering coefficient of most soils since this is due to the variation in the amount of light nuclei present, primarily oxygen but also carbon and, to a lesser extent, nitrogen. It is these nuclei rather than the heavier ones such as silicon, aluminium, iron, etc. which will affect the slowing down properties of the soil and hence the thermal flux at the detector.

The spectrum used for the fast source was that reported by Medveczky [1961] for a radium-beryllium source. This should be similar to other α,n sources, but some differences must be expected since the spectrum depends not only on the α source but, to some extent, on the size of the source itself [Anderson and Bond 1963; Thompson and Tayler 1965; Anderson and Neff 1972]. It is also reasonable to expect that the dependence of the thermal flux on the parameters ω, ρ, S_a and S_s would be little changed if the source were a fission neutron source such as ^{252}Cf. The source energy spectrum condensed over the top five energy groups used is shown in Figure 3.

A soil-water mixture with resonance absorption properties was achieved by adding varying concentrations of either cobalt or molybdenum to a specified SiO_2-water mixture. Cobalt has marked resonance absorption in the energy range 30 to 500 eV, while the major part of the resonance absorption cross section for molybdenum spans the wider range of about 30 to 800 eV and has smaller and somewhat more widely spaced resonance peaks than has cobalt. The position of the lowest energy resonance in molybdenum at 45 eV is lower than that in cobalt which is at 132 eV, while its ratio of resonance to thermal absorption is larger than that for cobalt which has, at 37.2 barns, a comparatively high thermal mass absorption coefficient. The behaviour of the resonance absorption and thermal absorption coefficients of these two elements spans, in a reasonable way, the behaviour of the absorption coefficients of other resonance absorbers likely to be found in soils in appreciable concentrations and hence are reasonable elements to choose when investigating the effect of resonance absorption on the performance of a neutron moisture meter. Moreover, the coefficients for these two elements are well documented in nuclear data libraries.

3. RESULTS AND DISCUSSION

The variation of the thermal flux at the detector position as the water content, the density and the thermal absorption coefficients of the 'soil' vary is shown in Table 5 for three different values of the matrix mass scattering coefficient. Note that this thermal flux, which is proportional to the count rate from a neutron moisture meter, is specified within an arbitrary scale factor. The way in which the probe response varies with these parameters is discussed in some detail below, together with some discussion on the response of the probe to both the presence of resonance capture and variations in the source-detector separation.

3.1 The Effect of Source-detector Separation

As expected, the highest count rate in the detector occurs with the source and detector coincident (Figure 4a). However, while some types of neutron moisture meter are constructed with source and detector coincident, or nearly so, others (see, for example, Figure 2) have the detector separated from the source. Although an increase in this separation clearly decreases the count rate in the detector, and hence the sensitivity of the probe, it does, as discussed below, improve some other properties of the probe.

Figures 4b,c and d show the count rate in the detector as a function of water concentration, for various source-detector separations and a variety of S_t values. It can be seen that, as noted previously [Wozniak 1973; Olgaard and Haahr 1967], there are significant changes in the slopes and shapes of the curves as the source-detector separation varies. Examination of these relationships enables a separation to be chosen which results in a closely linear response for the neutron moisture meter. While it is clear that such linearity does not hold for all mass absorption coefficients, Figures 4b,c and d show clearly that, if a separation of 9.59 cm were used, the assumption of linearity would not introduce significant errors as long as S_a is between 0.00171 and 0.006305 $cm^2\ g^{-1}$; even with S_a as large as 0.0189 $cm^2\ g^{-1}$, the maximum error introduced would be only ± 3 per cent. A source-detector separation of 5.74 cm was used in all other calculations, this being close to the source-detector separation in the probe used by Daniel et al. [1980].

3.2 The Importance of Resonance Capture

Table 2 presents values of the non-1/v resonance mass absorption coefficients for cobalt appropriate to the energy group that spans its resonance region, and shows how the magnitude of the resonance mass absorption coefficient is modified by changes in both cobalt concentration and water density for soils of representative matrix density and thermal neutron mass absorption coefficient. The table also shows the factor by which the group coefficient had to be multiplied to yield the correct value for the total 1/v and non-1/v absorption in the resonance group.

Figure 5a shows the extent to which the flux at the detector position decreases with increasing concentrations of cobalt in the soil-water-cobalt mixture when proper account is taken of resonance absorption in the cobalt, while Figure 5b shows the percentage error that would arise in an estimation of the water density if resonance absorption were ignored. In these calculations the thermal mass absorption coefficient of the matrix S_a prior to addition of the cobalt was the same as that for the calculations presented in Table 2. Figure 5b shows that the error in the water content is less than 2 per cent, even at cobalt densities as high as 10^{-2} g cm^{-3}. Apart from the fact that such levels would constitute significant mineralisation, such a cobalt concentration would add appreciably to the thermal mass absorption coefficient of the soil. For example, a cobalt concentration of 1 mg g^{-1} adds about 10 per cent to the magnitude of S_a for a dry SiO_2 matrix.

Table 3 and Figure 6 present the results of similar calculations for molybdenum as the resonance absorber. The concentrations chosen for molybdenum were those that gave the same S_a for the soil-molybdenum mixtures as for the soil-cobalt mixtures. The fact that the molybdenum concentrations are higher than the cobalt concentrations largely reflects the fact that the thermal neutron microscope absorption cross section for molybdenum is smaller than that for cobalt (see Table 4). Figure 6b shows that the error in the water content, which results from ignoring resonance capture when molybdenum is the resonance absorber, is ≤ 1.2 per cent compared to ≤ 0.3 per cent in the case of cobalt when they are present in concentrations that would increase S_a for a dry, SiO_2 matrix by about 10 per cent. The error at the concentration, which would correspond to an approximate doubling of S_a for a dry, SiO_2 matrix, is at most about 5.5 per cent.

It is clear from the above that systematic errors of a few per cent could arise in the value of the water content estimated from neutron moisture meter data if the effects of high concentrations of resonance absorbers were ignored. It is useful, then, to have some means of assessing whether or not resonance absorbers are present in high concentrations and some recipe for estimating the errors likely to arise if the presence of a particular absorber is ignored.

Table 4 indicates that most of the elements with high resonance absorption cross sections are 'minerals' and, hence, their presence in concentrations high enough to warrant concern would correspond to mineralisation of the region in which the neutron moisture meter measurements were made. Furthermore, Table 4 shows that elements with high resonance absorption also tend to have high thermal neutron absorption cross sections and so their presence in high concentrations leads to a high value of S_a. As pointed out below, the soil S_a is an important parameter which must be known if absolute water content values are to be derived from neutron moisture meter readings.

Figures 5b and 6b and the ratios of $RI/\sigma_a(th)$ from Table 4 suggest that the error in the water content, consequent on ignoring the effect of resonance absorption, is approximately proportional to $RI/\sigma_a(th)$. This provides a rough guide for estimating the effect of ignoring resonance absorption. For example, if we suspect the presence of caesium ($RI/\sigma_a(th) \sim 14$) in quantities which would contribute the same amount to S_a as 245 mg cm^{-3} of molybdenum, then the expected error in the water content would be $5.5 \times 14/8 \sim 10$ per cent compared to ~ 5.5 per cent for molybdenum with an $RI/\sigma_a(th)$ of ~ 8.

3.3 Variation of Probe Response as a Function of Water Density ω

As expected on the basis of both age diffusion theory and Olgaard's [1965] three-group diffusion theory calculations, the probe response is not, in general, a linear function of the water density. Examination of Figures 7 to 11, however, shows that, at each matrix density, the curves are more nearly straight lines as the water density increases. This trend is more pronounced as the matrix density increases and as the mass absorption coefficient decreases.

A systematic error in the estimate of the water content of the soil obtained from the moisture meter reading will result if a linear response is assumed. The magnitude of this error clearly depends on the magnitudes of the matrix density, the soil water content and the thermal neutron mass absorption coefficients of the soil, but for ρ between 1.0 and 1.667 g cm^{-3}, S_a between 6.3×10^{-3} and 18.9×10^{-3} cm^2 g^{-1}, and ω between 0.2 and 0.3 g cm^{-3}, it varies between about 2 per cent and 10 per cent.

3.4 Probe Response as a Function of the Mass Absorption Coefficient S_a

Figures 12 to 16 show that the change in the probe response as a function of the thermal neutron mass absorption coefficient is quite marked and also non-linear. The curves in Figures 12 to 16 also show that the fractional decrease in the count rate with increasing absorption increases as water density decreases. This is to be expected because the comparatively large thermal neutron mass absorption coefficient of water, 22.2×10^{-3} cm^2 g^{-1}, will mask the effect of increasing matrix absorption when the water density is high.

Increasing water density in the matrix surrounding the detector also modifies the neutron energy spectrum and hence the effective neutron mass absorption coefficient. At a matrix density of 1.0 g cm^{-3}, the neutron mass absorption coefficient in the thermal group increases by 2 per cent at the lowest S_a, and by less than 1 per cent at the highest S_a as the water density increases from 0.1 to 0.4 g cm^{-3}, while at the highest matrix density the increases are 1.5 and 2 per cent. These small changes indicate that, although there is a spectrum shift as the water density changes, the shift has a comparatively small effect on the group-averaged coefficients.

3.5 The Effect of Changes in the Matrix Mass Scattering Coefficient S_s

From Figures 17 and 18 it can be seen that the flux at the detector increases with increasing matrix mass scattering coefficient. This is to be expected, as increases in the scattering coefficient will have a similar effect on neutron transport processes as small changes in the water content. As with changes in S_a, changes in the mass scattering coefficient S_s lead to the greatest fractional changes in the estimated water content when the water content is lowest. This fractional change is also greater the lower is S_a. A 5 per cent change in the mass scattering coefficient leads to an apparent change in the water content that varies from about 1 to 11 per cent as S_a, ρ and ω vary from 1.71×10^{-3} cm^2 g^{-1}, 1.0 g cm^{-3} and 0.4 g cm^{-3} to 18.9 cm^2 g^{-1}, 2.0 g cm^{-3} and 0.1 g cm^{-3}. As the variation in the mass scattering coefficient of soils is typically about 10 per cent, an uncertainty of about 1 to 11 per cent would be introduced into the value of the water content estimated from a neutron moisture meter reading if the effect of changes in this parameter were completely neglected.

Unlike the mass absorption coefficient, where small fractions of large absorbers can have a considerable effect on the macroscopic cross section, the main contribution to the mass scattering coefficient comes from the major components in the matrix. This means that, if the proportions of the major constituents can be determined, e.g. by chemical analysis (in particular oxygen, silicon, iron, magnesium, aluminium and carbon), the uncertainty in the probe response due to uncertainty in the mass

scattering coefficient can be reduced to insignificant levels.

3.6 Probe Response as a Function of Matrix Density

It can be seen from Figures 19 to 23 that, over almost the whole range of parameters considered, the probe response increases linearly with matrix density, but that the slope of the line decreases as the matrix absorption increases. However, at the highest absorptions the relationship between probe response and matrix density is no longer linear.

Therefore, over most of the range of the parameters the response can be represented as

$$R(\rho, S_a, \omega) = \rho M(\omega, S_a) + C(\omega, S_a). \tag{5}$$

Figures 24a and b show the slope M and the intercept C as functions of the absorption S_a for fixed water density ω, and Figures 25a and b show the slope and intercept as functions of water density for fixed absorption. It can be seen from Figure 24a that the slope decreases monotonically with increasing absorption and that the slopes at different water content get closer together and intercept as absorption increases. Figure 25a shows that, although at the lower absorptions the slope increases with increasing water density, it decreases with increasing water density at higher absorptions. It is also clear from Figures 24a and 25b that, for S_a and ω greater than about 8×10^{-3} cm^2 g^{-1} and 0.1 g cm^{-3} respectively, a crude representation of the probe response would be

$$R(\rho, S_a, \omega) = \rho M(S_a) + C(\omega) \ . \tag{6}$$

The range of applicability of this expression is not too restrictive with respect to ω. But soils with S_a greater than 8×10^{-3} cm^2 g^{-1} are relatively uncommon.

Using experimental measurements, other workers have found that reasonable corrections for density variation can be made by an empirical rule. For example Olgaard [1965] derived

$$\frac{\partial \phi}{\partial \rho} = k\omega + C \tag{7}$$

where ϕ is the count rate, ω the concentration of water, k and C are constants which are slightly different for different soils: while Greacen and Schrale [1976] derived

$$\phi_s = \phi_r(\rho_s / \rho)^P \tag{8}$$

where ϕ_s is the count rate which would be obtained with a standard density ρ_s calculated from the observed count rate ϕ_r in soil density ρ. The index P is a constant which varies from soil to soil but using P = 0.5 for all soils did not produce a value which was significantly different from that obtained using the optimum value of P.

Neither of the empirical expressions (7) and (8) are consistent with approximate expression (6) or with the results presented in Figures 7 to 11. In particular, the fractional index that appears in expression (8) is a surprise and hard to understand when the way neutrons interact with matter is considered.

4. CONCLUSIONS

Resonance capture affects the response of a neutron moisture meter only when elements, having significant resonance capture, such as the rare earths, cobalt, manganese, zinc, etc., are present in the soil in concentrations which would be reflected in a high thermal mass absorption coefficient or in signficant mineral content of the soil. The implication is that, apart from a few exceptions, the neutron capture properties of a soil can be characterised by a thermal neutron mass absorption coefficient which need not be identified with any particular nucleus. Such a cross section is best measured by some nuclear technique [for example, McCulloch and Wall 1976], as the mass absorption coefficient can be influenced by small proportions of high neutron absorbers, such as boron, which are expensive and inaccurate to determine by chemical analysis.

Even when neutron moisture meters are used to determine the water content of mine overburden heaps [for example, Daniel et al. 1980] materials with high resonance capture are unlikely to be present in concentrations great enough to warrant taking resonance capture effects into account. Such effects cannot always be neglected. If attempts were made to measure the water content in and around a uranium ore body containing the mineral xenotime which contains the elements Sm, Eu, Gd, Dy, Ho, Er, Yb, Th and U, the concentration of Gd alone would make it impossible to analyse sensibly any neutron moisture meter data.

The differing composition of soils can lead to a variability of about ± 5 per cent in the mass scattering coefficient of the matrix. This, in turn, can lead to apparent changes of water content by up to about 10 per cent, depending on the magnitude of such parameters as matrix density, thermal neutron mass absorption coefficients and the water content itself. Fortunately, the mass scattering coefficients of most elements are of similar magnitude and the bulk of the matrix mass scattering coefficient is made up by a few elements. It is therefore possible to reduce the uncertainty in the mass scattering coefficient, and hence in the estimated water content to the extent required, by resort to comparatively inexpensive chemical analysis.

This leaves the water density, matrix density and thermal neutron mass absorption coefficient as the main variables on which the response of the neutron moisture meter depends. Over much of the range the response depends linearly on the matrix density ρ and can be written as

$$R(\rho, S_a, \omega) = \rho M(\omega, S_a) + C(\omega, S_a) \quad .$$

As the dependence of M on S_a and C on ω is much less marked than their dependences on ω and S_a, a crude representation of the response for $S_a > 8 \times 10^{-3}$ cm^2 g^{-1} and $\omega > 0.1$ g cm^{-3} is

$$R(\rho, S_a, \omega) = \rho M(S_a) + C(\omega) \quad .$$

It is possible that for some applications this relationship is sufficiently accurate.

However, the detector response is, in general, a non-linear function of ρ, S_a and ω over the range of variability that these parameters have in most practical applications. Fortunately, this function is sufficiently slowly varying, and access to computers is now so common, that application of simple polynomial fits to the data presented here provides a practical method of interpolation to find the response for values of ρ, S_a, S_s and ω that pertain to a given situation [see, for example, Wilson 1983].

5. ACKNOWLEDGEMENTS

It is a pleasure to record the assistance and instruction given by Dr J. Pollard and Mr G. Robinson in the use of some of the computer codes used in this report. Without this guidance the setting up of the models would have been extremely tedious.

6. REFERENCES

Anderson, M.E. and Bond, W.H. [1963] - Neutron spectrum of a plutonium-beryllium source. Nucl. Phys., 43:330-338.

Anderson, M.E. and Neff, R.A. [1972] - Neutron energy spectra of different size ^{239}Pu-Be(α,n) sources. Nucl. Instrum. Methods, 99:231-238.

Andrieux, C., Buscarlet, L., Guitton, J. and Merite, B. [1962] - Mesure en profondeur de la teneur en eau des sols par ralentissement des neutrons rapides. Proc. Symp., Bombay, 26 February-2 March. IAEA, Vienna, pp. 187-219.

Ballard, L.F. and Ely, R.L [1961] - Moisture determination in corn by neutron moderation. ORO-485.

Daniel, J.A., Harries, J.R. and Ritchie, A.I.M. [1980] - Water movement caused by monsoonal rainfall in an overburden dump undergoing pyritic oxidation. In *Biogeochemistry of Ancient and Modern Environments* (Eds. Trudinger, P.A., Walker, M.R., Ralph, B.J.). Aust. Acad. Sci., Canberra, pp.623-629.

Gardner, W. and Kirkham, D. [1952] - Determination of soil moisture by neutron scattering. Soil Sci., 391:73-74.

Glasstone, S. and Edlund, M.C. [1958] - The elements of nuclear reactor theory. Van Nostrand, Princeton.

Greacen, E.L. and Schrale, G. [1976] - The effect of bulk density on neutron meter calibration. Aust. J. Soil Res., 14:159-169.

Hearst, J.R. [1968] - Effects of medium variations on the measurement of in situ hydrogen content. Geophys., 33, 4:657-667.

Hearst, J.R. [1974] - Neutron logging in partially saturated media. Proc. Int. Seminar on Instruments and Systems for Measuring and Monitoring Water Quality and Quantity, Chicago.

Holmes, J.W. [1956] - Calibration and field use of the neutron scattering method of measuring soil water content. Aust. J. Appl. Sci., 7:45-58.

Honek, H.C. [1964] - ENDF - evaluated nuclear data file description and specifications. BNL 8381.

Honig, A., Pospisilová-Rothscheinová, Ludmila, Kablena, P. and Habarta, J. [1971] - Commercial portable gauges for radiometric determination of the density and moisture content of building materials - a comparative study. IAEA, Vienna, Technical Report Series No.130.

Jakeman, D. [1966] - Physics of Nuclear Reactors. English Universities Press, London.

McCulloch, D.B. and Wall, T. [1976] - A method of measuring the neutron absorption cross sections of soil samples for calibration of the neutron moisture meter. Nucl. Instrum. Methods. 137:577-581.

Medveczky, L. [1961] - Be(α,n) Neutronforrások Energiaspektruma. Atomki Kozlemenyek 3:2-3, Debreceu, Hungary.

Mughabghab, S.F. and Garber, D.I. [1973] - Neutron cross sections, Vol.I: Resonance parameters. BNL-325, Vol.I, 3rd Ed., National Neutron Cross Section Center, Brookhaven National Lab.

Olgaard, P.L. [1965] - On the theory of the neutronic method for measuring the water content in soil. Riso Report No.97. Danish Atomic Energy Commission.

Olgaard, P.L. and Haahr, V. [1967] - Comparative experimental and theoretical investigations of the DM neutron moisture probe. Nucl. Eng. Des., 5:311-324.

Pollard, J.P. [1974] - AUS module POW - A general purpose 0, 1 and 2D multigroup neutron diffusion code including feedback-free kinetics. AAEC/E269.

Robinson, G.S. [1975] - AUS - The Australian modular scheme for reactor neutronics computations. AAEC/E369.

Robinson, G.S. [1980] - Private communication.

Robinson, G.S. [1977] - AUS module MIRANDA - A data preparation code based on multi-region resonance theory. AAEC/E410.

Semmler, R.A. [1963] - Neutron moderation moisture meters. Analysis of application to coal and soil. Final report COO-712-73 (September).

Thompson, M.N. and Taylor, J.M. [1965] - Neutron spectra from Am-α-Be and Ra-α-Be sources. Nucl. Instrum. Methods. 37:305-308.

Weast, R.C. (Editor in Chief) [1967-1968] - Handbook of Chemistry and Physics. 48th Edition. Chemical Rubber Co., Cleveland, Ohio.

Weinberg, A.M. and Wigner, E.P. [1958] - The Physical Theory of Neutron Chain Reactors. University of Chicago Press, Chicago.

Wilson, D.J. [1983] - Nuclear moisture meters: The effects of various soil parameters. Nucl. Tech., 60:155-163.

Wozniak, J. [1973] - Calibration of neutron gauges for measuring the soil moisture content in the 4π geometry. IJJ 27/1, Poland Institute of Nuclear Techniques.

Zuber, A. and Cameron, J.F. [1966] - Neutron soil moisture gauges. At. Energ. Rev., 4, 143-166.

TABLE 1
GROUP STRUCTURE USED IN THE POW CALCULATION
[Pollard 1974]

Group	Energy Range
1	15 MeV - 6.065 MeV
2	6.065 MeV - 4.724 MeV
3	4.724 MeV - 2.865 MeV
4	2.865 MeV - 1.738 MeV
5	1.738 MeV - 302.0 keV
6	302.0 keV - 0.414 eV
7	0.414 eV - 0.001026 eV

Extra groups inserted for resonance calculation
Cobalt 583 eV - 37.3 eV
Molybdenum 748.5 eV - 2.051 eV

TABLE 2
RESONANCE ABSORPTION DATA FOR COBALT

'Resonance' group covered the energy range 583 eV to 37.3 eV.
Matrix used was SiO_2 at 1.6667 g cm^{-3}
with S_a (thermal) 6.305 x 10^{-3} cm^2 g^{-1}

	Co at 0.001 g cm^{-3}		Co at 0.01 g cm^{-3}	
Water Content (g cm^{-3})	Above 1/v RI barns	Factor by which to multiply S_a of resonance group	Above 1/v RI barns	Factor by which to multiply S_a of resonance group
0.1	55.5661	9.1172	40.1581	42.9131
0.2	56.9477	9.2515	44.2014	46.8570
0.3	57.6622	9.3213	46.6924	49.2901
0.4	58.1005	9.3640	48.4361	50.9930

RI = Resonance integral: at infinite dilution this is 60.2273 barns

TABLE 3
RESONANCE ABSORPTION DATA FOR MOLYBDENUM

'Resonance' group covered the energy range 748.5 eV to 2.051 eV
Matrix used was SiO_2 at 1.6667 g cm^{-3}
with S_a (thermal) = 6.305 x 10^{-3} cm^2 g^{-1}

Water Content (g cm^{-3})	Mo at 0.0245 g cm^{-3}		Mo at 0.245 g cm^{-3}	
	Above l/v RI barns	Factor by which to multiply S_a of resonance group	Above l/v RI barns	Factor by which to multiply S_a of resonance group
0.1	19.8209	9.05382	10.3246	31.6291
0.2	21.2318	9.43152	11.8649	35.7745
0.3	22.0937	9.66289	13.0257	38.9007
0.4	22.6779	9.81989	13.9590	41.4247

RI = resonance integral; at infinite dilution this is 26.0726 barns

TABLE 4
SOME ELEMENTS HAVING SIGNIFICANT RESONANCE INTEGRALS

Element	Microscopic Thermal Absorption Cross Section σ_a(th) barns	Resonance Integral* RI barns	Energy at First Resonance* (eV)	Abundance in Earth's Crust† (g/t av.)
Co	37.2	75.5	132	23
Zn	1.1	2.3	530	132
Ga	1.68	15.6	95	15
Ge	2.3	6.1	105	7
As	4.3	60	47	5
Br	6.8	90	35.6	1.6
Nb	1.15	8.5	35.9	24
Mo	2.65	22	45	15
Sn	0.63	6.1	39.4	40
Sb	5.4	175	6.24	1
Cs	29	415	5.9	7
Ba	1.2	7.5	24.5	250
Sm	5800	1400	0.1	6.5
Eu	4600	2430	0.327	1.1
Gd	49000	390	2.01	6.4
Dy	930	1600	2.72	4.5
Ho	66.5	700	12.8	1.2
Er	162	740	0.47	2.5
Yb	36.6	182	0.597	2.7
Hf	102	2000	30.5	4.5
W	18.5	352	4.14	69
Th	7.4	70	21.7	12
U	7.6	280	6.68	4

* Mughabghab and Garber [1973] † Weast [1967-68]

TABLE 5
VARIATION OF THERMAL FLUX AT THE DETECTOR POSITION
AS A FUNCTION OF MATRIX DENSITY ρ, WATER DENSITY ω,
THERMAL MASS ABSORPTION COEFFICIENT S_a
AND MASS SCATTERING COEFFICIENT S_s

Mass scattering coefficient $S_s = 0.10844$ cm^2 g^{-1} (no added carbon)

Absorption S_a (cm^2 g^{-1})	Water Density ω (g cm^{-3})	Matrix Density ρ (g cm^{-3})				
		0.5	1.000	1.333	1.667	2.000
1.7088×10^{-3}	0.1	1.0144	1.7621	2.3064	2.8870	3.4971
	0.2	2.5661	3.8007	4.6479	5.5154	6.3961
	0.3	4.5134	6.2137	7.2970	8.3809	9.4579
	0.4	6.9308	8.8566	10.1097	11.3441	12.5522
3.418×10^{-3}	0.1	0.8651	1.4011	1.7802	2.1765	2.5882
	0.2	2.3136	3.2236	3.8201	4.4277	5.0283
	0.3	4.2361	5.4474	6.2221	6.9752	7.7083
	0.4	6.4949	7.9225	8.8146	9.6674	10.4827
6.305×10^{-3}	0.1	0.7034	1.0575	1.3044	1.5601	1.8230
	0.2	2.0102	2.6033	2.9889	3.3612	3.7441
	0.3	3.8021	4.5720	5.0521	5.5117	5.9525
	0.4	5.9423	6.8184	7.3486	7.8445	8.3097
12.613×10^{-3}	0.1	0.5041	0.6942	0.8284	0.9665	1.1073
	0.2	1.5708	1.8440	2.0323	2.2200	2.4053
	0.3	3.1159	3.3965	3.5918	3.7851	3.9727
	0.4	5.0193	5.2369	5.3961	5.5552	5.7090
18.914×10^{-3}	0.1	0.3939	0.5167	0.6050	0.6957	0.7878
	0.2	1.2928	1.4293	1.5379	1.6497	1.7612
	0.3	2.6443	2.7034	2.7832	2.8729	2.9653
	0.4	4.3488	4.2504	4.2565	4.2853	4.3243

TABLE 5 (Continued)
VARIATION OF THERMAL FLUX AT THE DETECTOR POSITION AS A FUNCTION OF MATRIX DENSITY ρ, WATER DENSITY ω, THERMAL MASS ABSORPTION COEFFICIENT S_a AND MASS SCATTERING COEFFICIENT S_s

Mass scattering coefficient $S_s = 0.12$ cm^2 g^{-1} (0.002104 x 10^{24} atoms C added to each gram of soil)

Absorption S_a ($cm^2\ g^{-1}$)	Water Density ω ($g\ cm^{-3}$)	Matrix Density ρ ($g\ cm^{-3}$)				
		0.5	1.000	1.333	1.667	2.000
1.7088 x 10^{-3}	0.1	1.0858	1.9365	2.5643	3.2364	3.9477
	0.2	2.6811	4.0589	5.0140	5.9952	6.9962
	0.3	4.7337	6.5358	7.7429	8.9522	10.1607
	0.4	7.1080	9.2244	10.6107	11.9766	13.3194
3.418 x 10^{-3}	0.1	0.9269	1.5429	1.9832	2.4463	2.9294
	0.2	2.4181	3.4497	4.1316	4.8198	5.5079
	0.3	4.3756	5.7320	6.6052	7.4565	8.2877
	0.4	6.6610	8.2527	9.2525	10.2106	11.1276
6.305 x 10^{-3}	0.1	0.7542	1.1663	1.4560	1.7573	2.0681
	0.2	2.1012	2.7841	3.2300	3.6707	4.1056
	0.3	3.9269	4.8116	5.3646	5.8940	6.4022
	0.4	6.0933	7.1020	7.7133	8.2852	8.8213
12.613 x 10^{-3}	0.1	0.5411	0.7672	0.9268	1.0913	1.2591
	0.2	1.6421	1.9737	2.1984	2.4215	2.6404
	0.3	3.2176	3.5750	3.8151	4.0492	4.2747
	0.4	5.1450	5.4539	5.6637	5.8621	6.0598
18.914 x 10^{-3}	0.1	0.4231	0.5708	0.6765	0.7852	0.8952
	0.2	1.3508	1.5289	1.6625	1.7980	1.9317
	0.3	2.7288	2.8435	2.9540	3.0708	3.1876
	0.4	4.4548	4.4231	4.4636	4.5216	4.5855

TABLE 5 (Continued)
VARIATION OF THERMAL FLUX AT THE DETECTOR POSITION AS A FUNCTION OF MATRIX DENSITY ρ, WATER DENSITY ω, AND THERMAL MASS ABSORPTION COEFFICIENT S_a AND MASS SCATTERING COEFFICIENT S_s

Mass scattering coefficient $S_s = 0.13$ cm^2 g^{-1} (0.0038987 x 10^{24} atoms C added to each gram of soil)

Absorption S_a (cm^2 g^{-1})	Water Density ω (g cm^{-3})	Matrix Density ρ (g cm^{-3})				
		0.5	1.000	1.333	1.667	2.000
1.7088 x 10^{-3}	0.1	1.1491	2.0934	2.7969	3.5538	4.3577
	0.2	2.7820	4.2872	5.3391	6.4233	7.5320
	0.3	4.8649	6.8185	8.1346	9.4569	10.7806
	0.4	7.2624	9.5459	11.0483	12.5315	13.9915
3.418 x 10^{-3}	0.1	0.9818	1.6706	2.1673	2.6918	3.2404
	0.2	2.5097	3.6423	4.4033	5.1692	5.9370
	0.3	4.4971	5.9820	6.9420	7.8812	8.7990
	0.4	6.8055	8.5410	9.6359	10.6857	11.6924
6.305 x 10^{-3}	0.1	0.7993	1.2645	1.5936	1.9371	2.2919
	0.2	2.1810	2.9442	3.4443	3.9397	4.4288
	0.3	4.0354	5.0218	5.6394	6.2314	6.7990
	0.4	6.2244	7.3493	8.0323	8.6708	9.2688
12.613 x 10^{-3}	0.1	0.5733	0.8319	1.0147	1.2031	1.3957
	0.2	1.7038	2.0861	2.3436	2.5979	2.8470
	0.3	3.3044	3.7287	4.0075	4.2775	4.5359
	0.4	5.2521	5.6394	5.8929	6.1346	6.3612
18.914 x 10^{-3}	0.1	0.4491	0.6204	0.7426	0.8681	0.9951
	0.2	1.4025	1.6184	1.7751	1.9323	2.0865
	0.3	2.8036	2.9684	3.1062	3.2478	3.3865
	0.4	4.5487	4.5761	4.6476	4.7314	4.8174

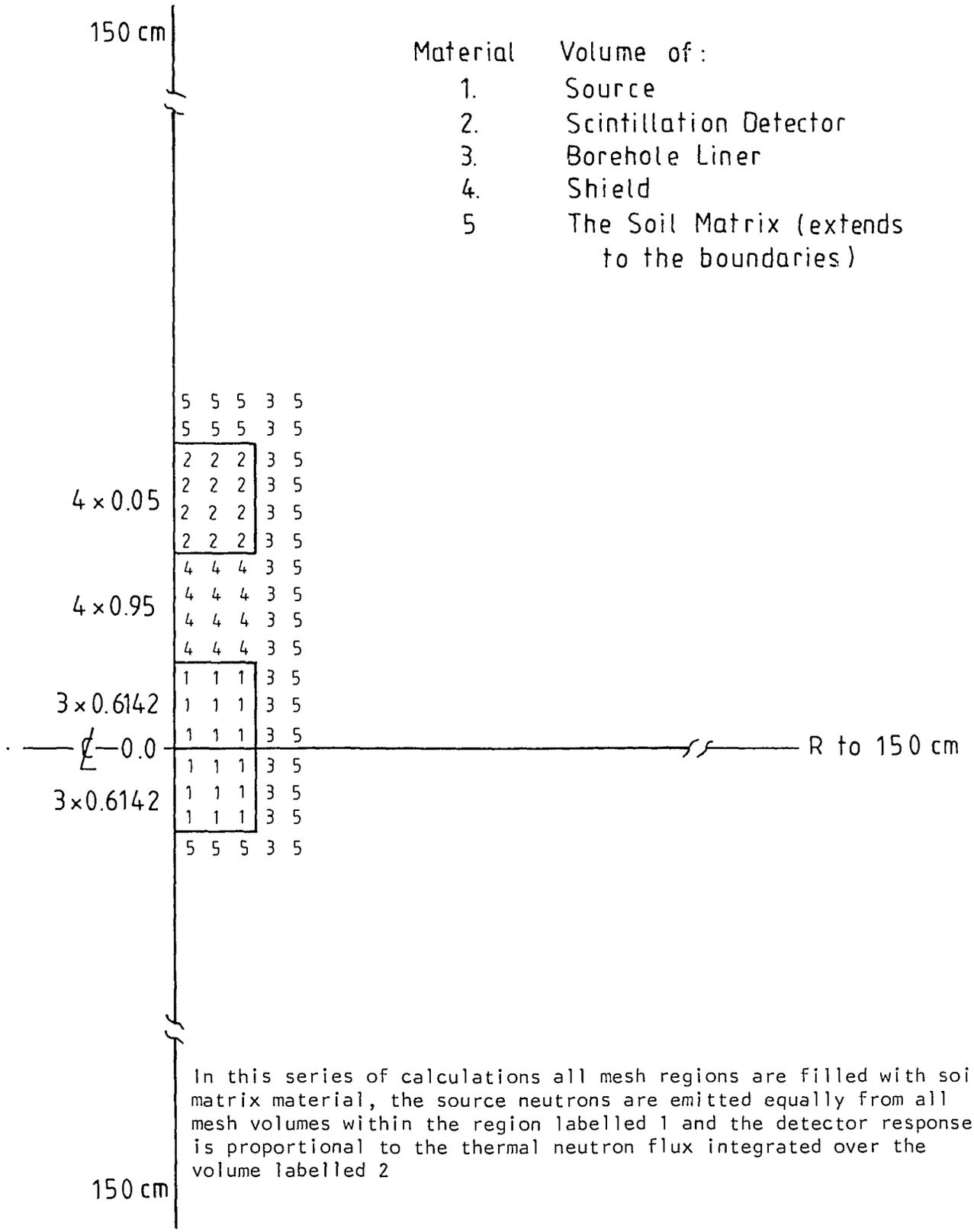

Figure 1 Geometry assumed for source detector and soil surrounding the detector in the diffusion theory calculation

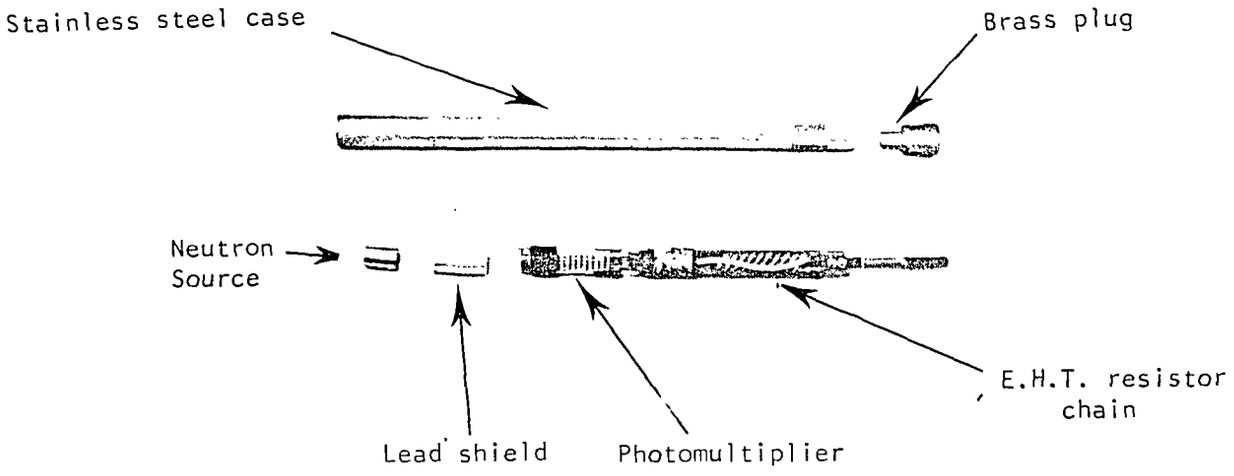

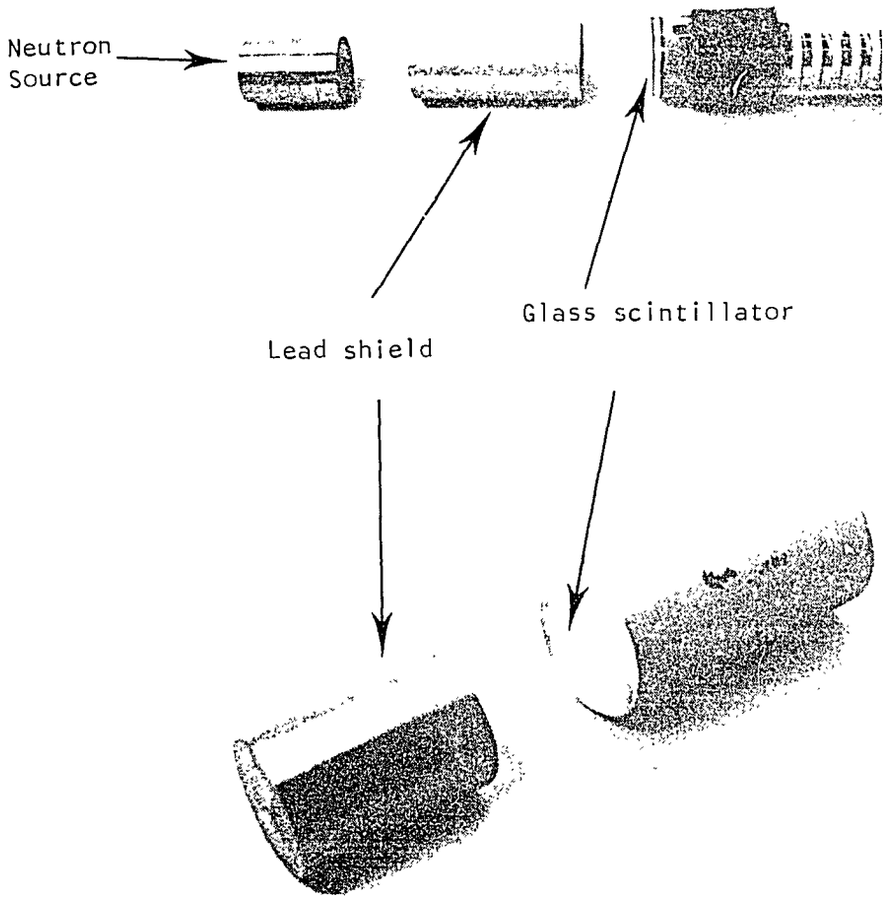

Figure 2 The construction of a typical neutron moisture meter probe. The stainless steel case is 390 mm long and 2.54 mm diameter.

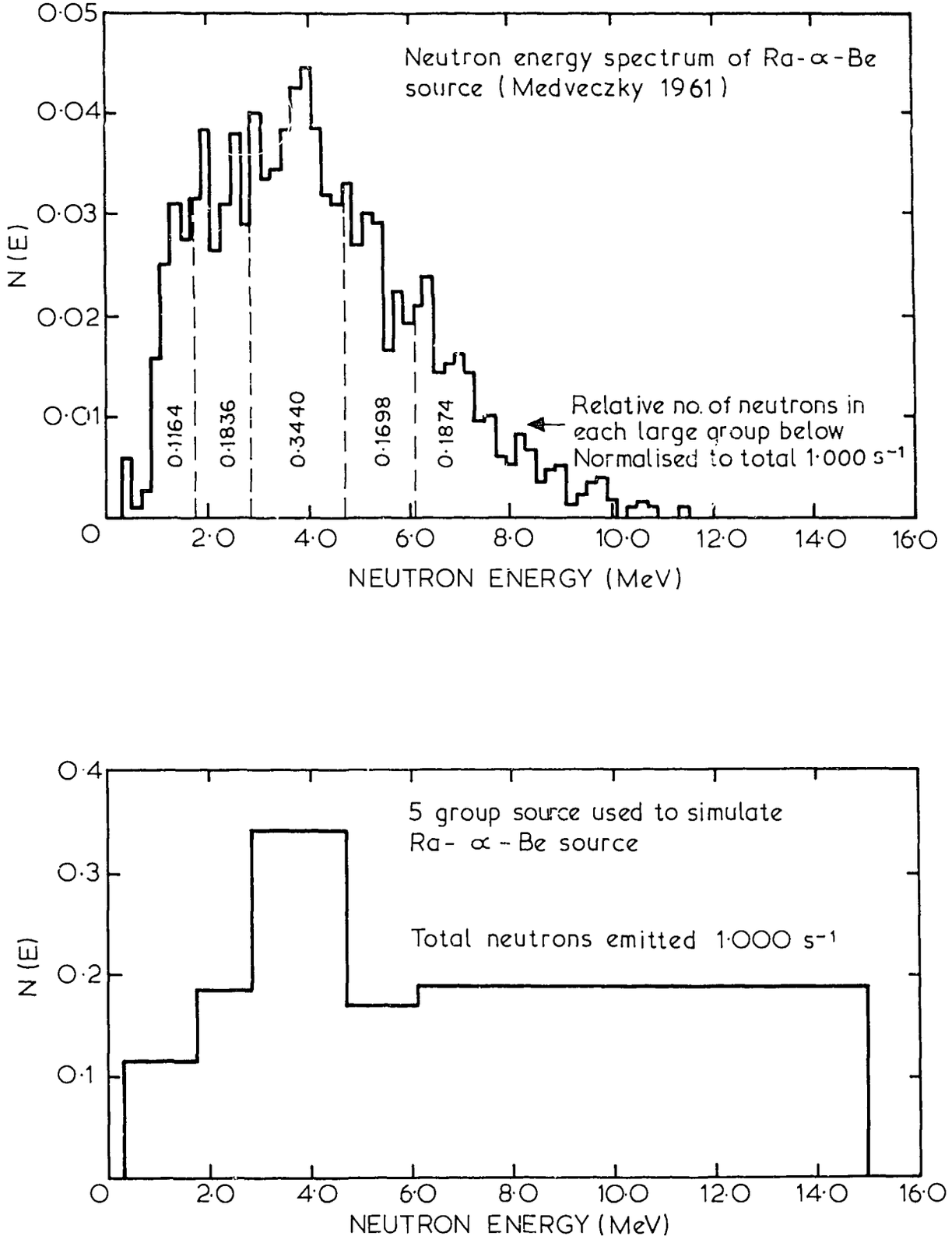

Figure 3 Energy spectrum of the neutron source used in the calculation

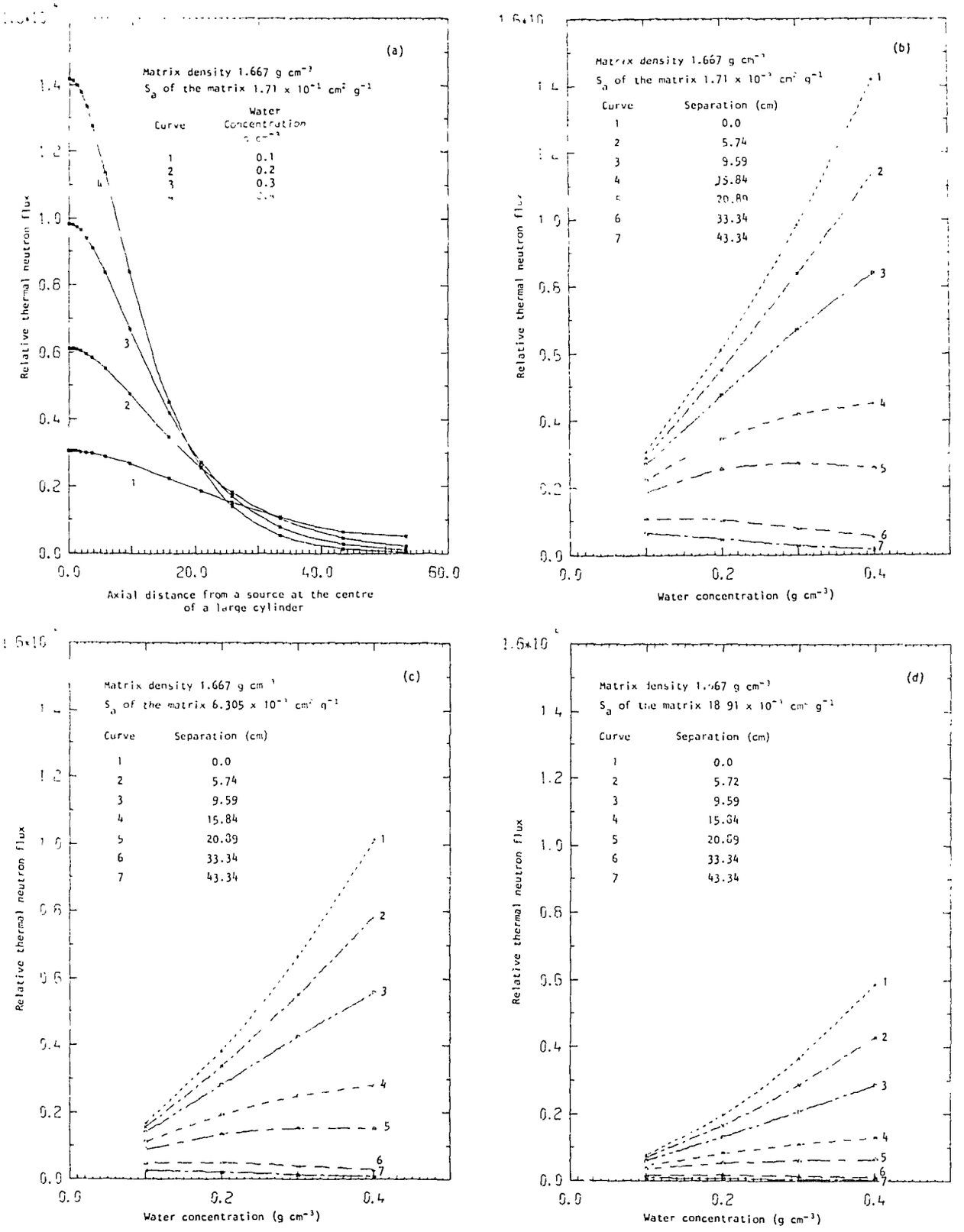

Figure 4a As a function of source-detector separation for various values of ω, S_a fixed at 1.7×10^{-3} $cm^2\ g^{-1}$

Figure 4b,c,d As a function of ω for various source-detector separations, S_a fixed at 1.7×10^{-3}, 6.31×10^{-3}, and 18.91×10^{-3} $cm^2\ g^{-1}$

Figure 4 Relative neutron flux at the detector as a function of source-detector separation, S_a and ω

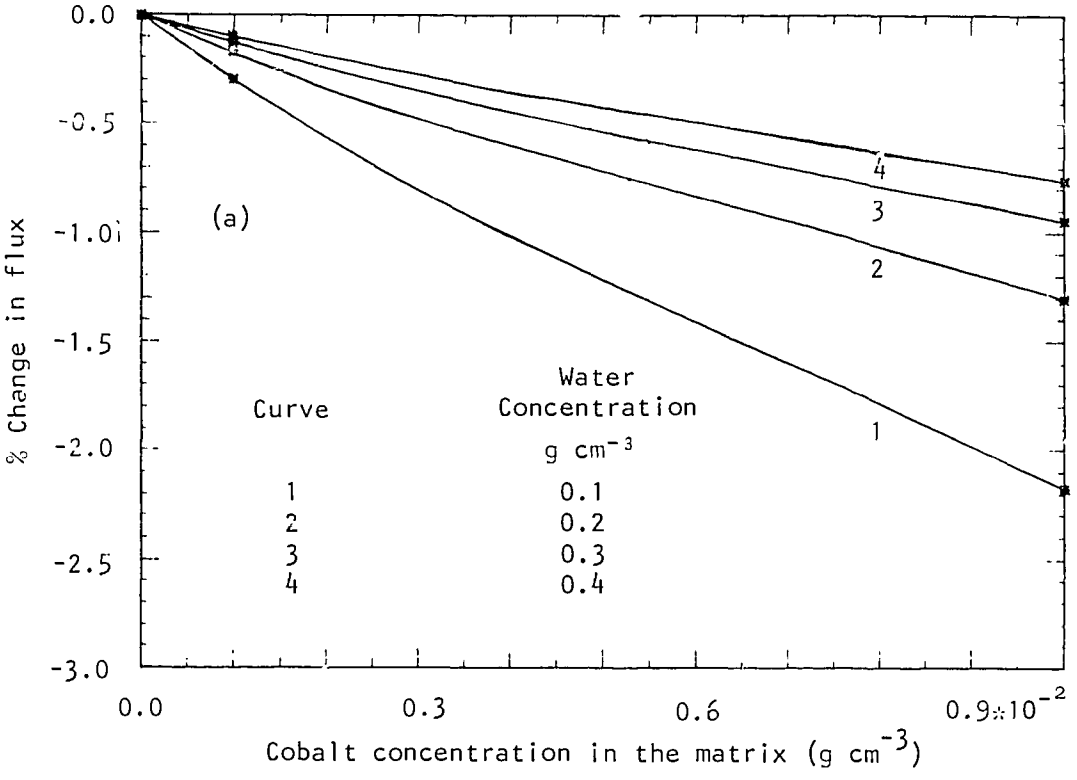

Figure 5a The percentage change in flux at the detector as a function of cobalt concentration if resonance absorption is ignored

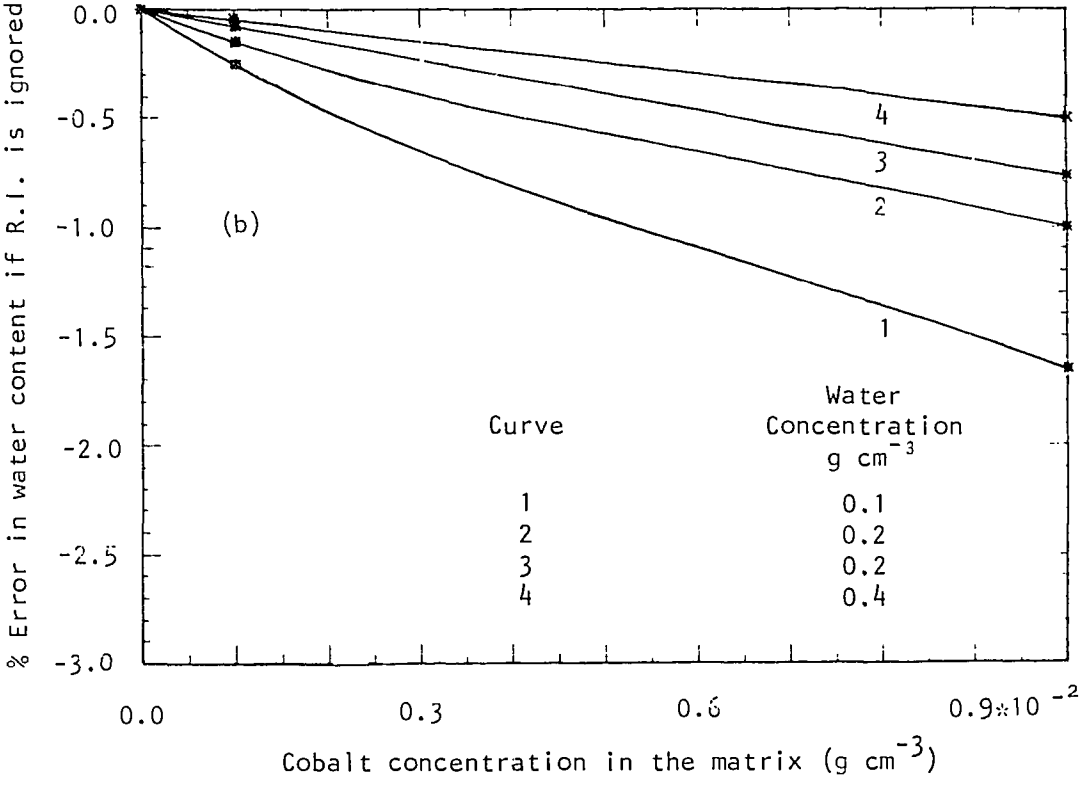

Figure 5b The percentage error in the water content as a function of cobalt concentration if resonance absorption is ignored

Figure 5 The effect of resonance capture on neutron moisture meter results in soils of different water content when cobalt is the resonant absorber

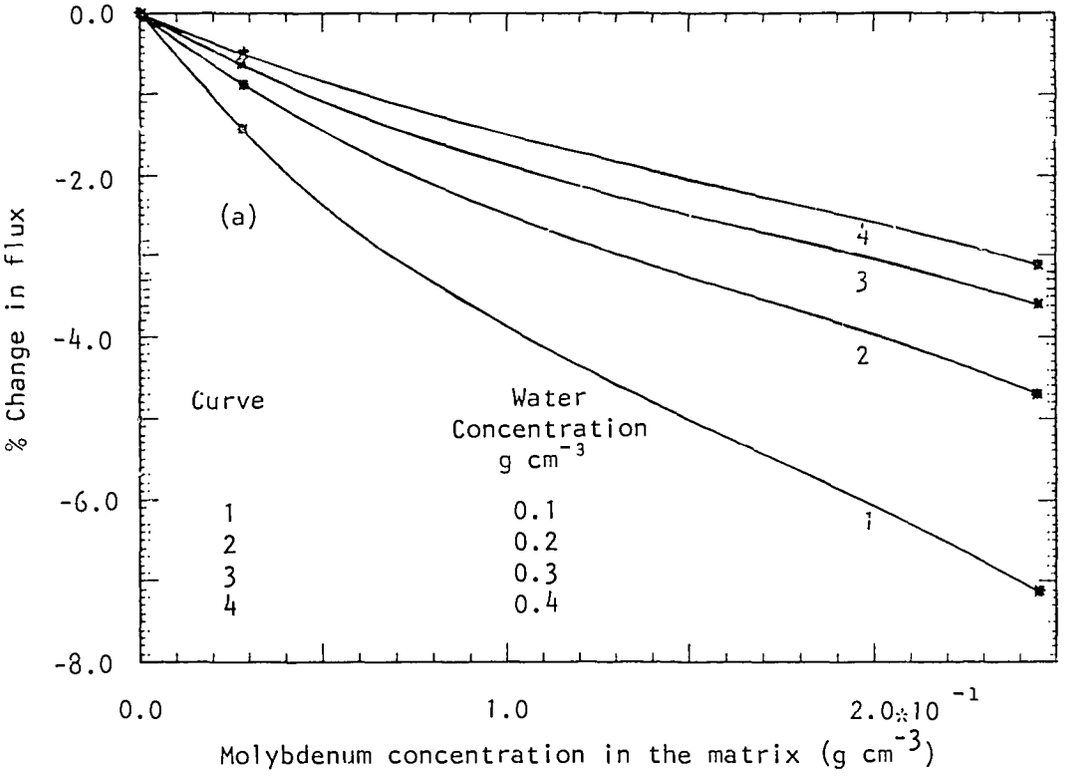

Figure 6a The percentage change in flux at the detector as a function of molybdenum concentration

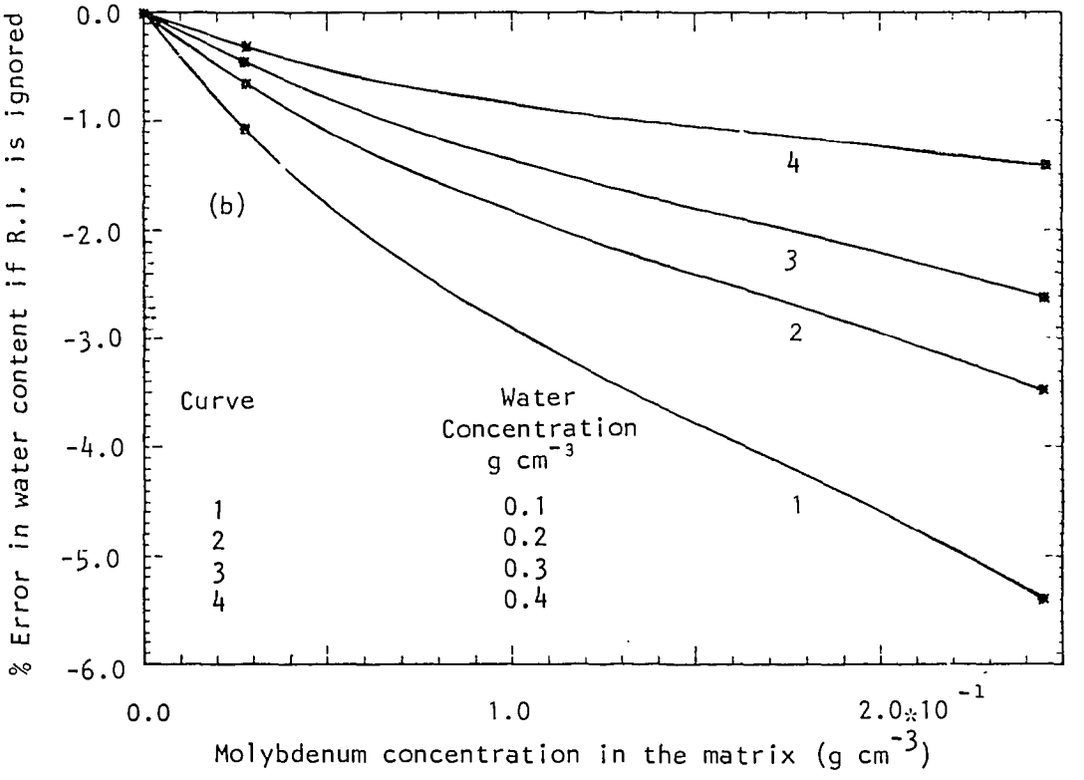

Figure 6b The percentage error in the water content as a function of molybdenum concentration if resonance absorption is ignored

Figure 6 The effect of resonance capture on neutron moisture meter results in soils of different water content when molybdenum is the resonant absorber

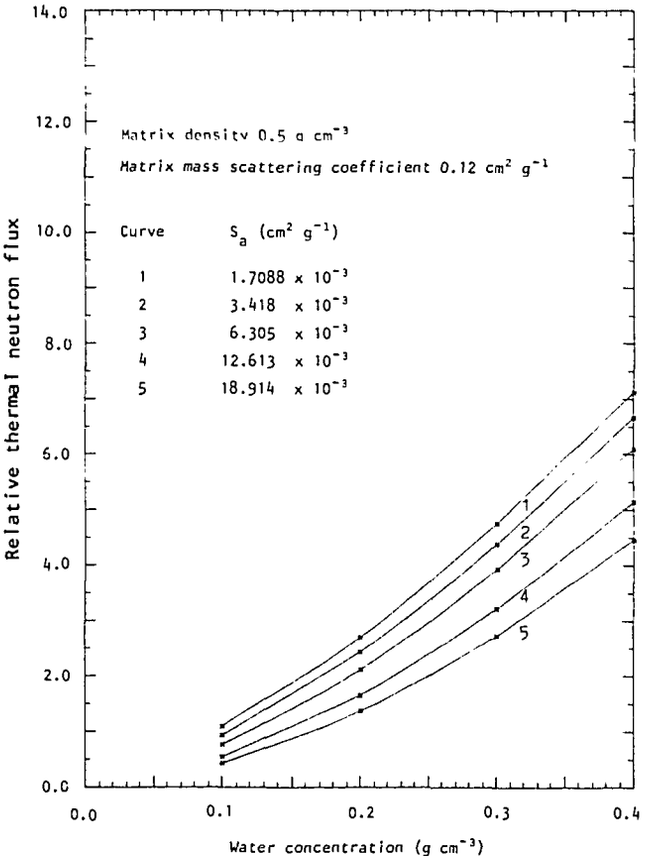

Figure 7 Detector response as a function of water content for various S_a; matrix density 0.5 g cm^{-3}

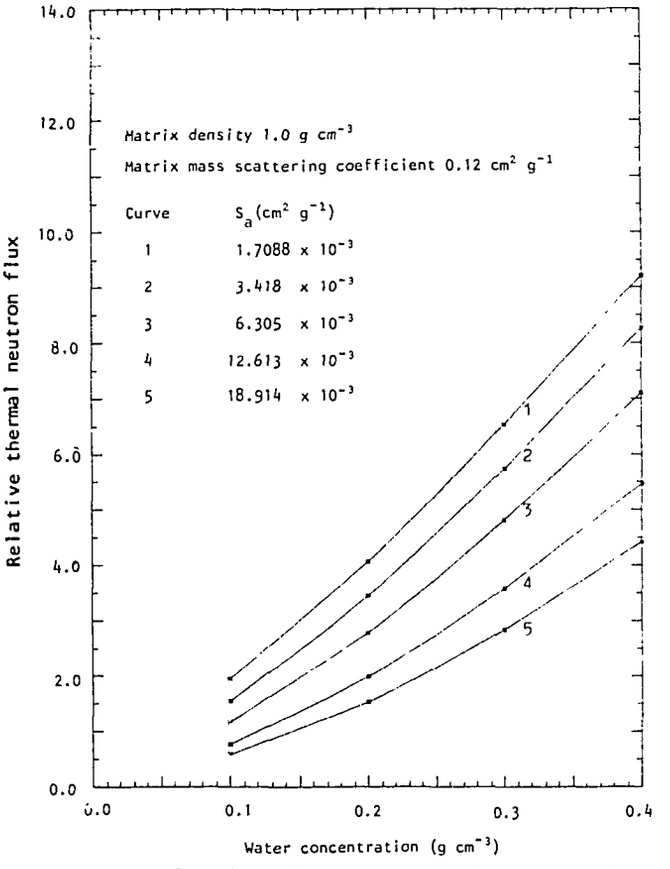

Figure 8 Detector response as a function of water content for various S_a; matrix density 1.0 g cm^{-3}

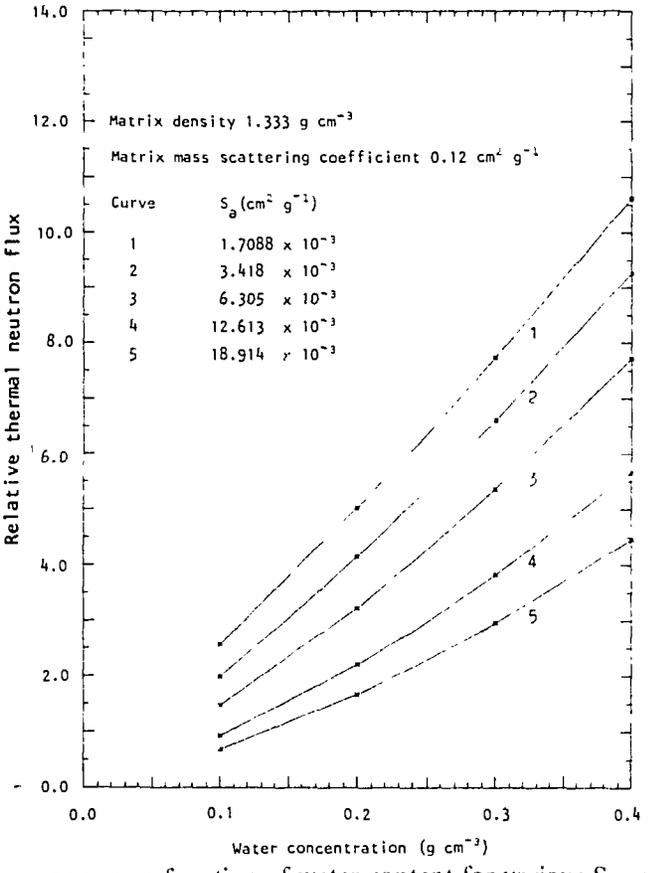

Figure 9 Detector response as a function of water content for various S_a: matrix density 1.333 g cm^{-3}

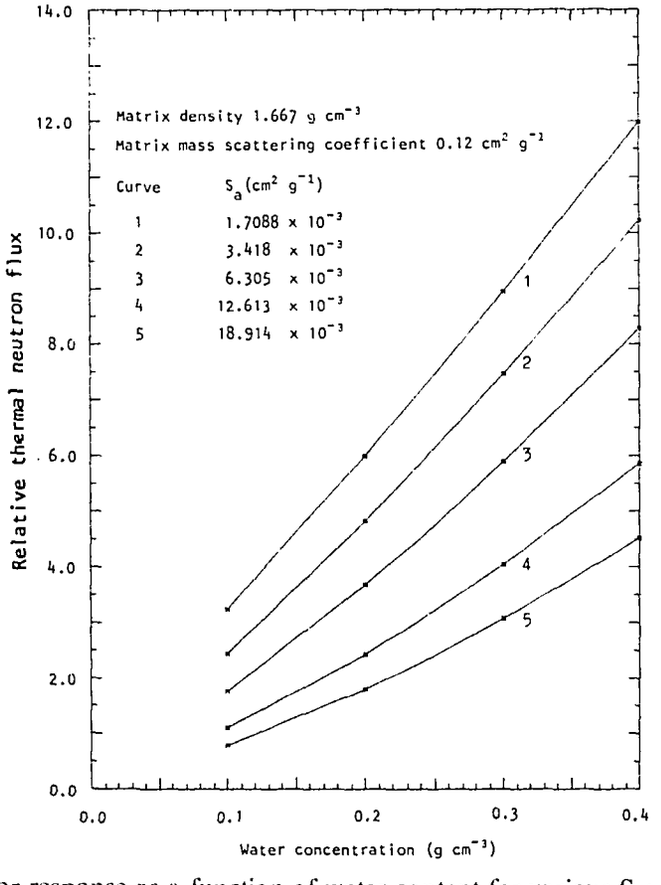

Figure 10 Detector response as a function of water content for various S_a: matrix density 1.667 g cm^{-3}

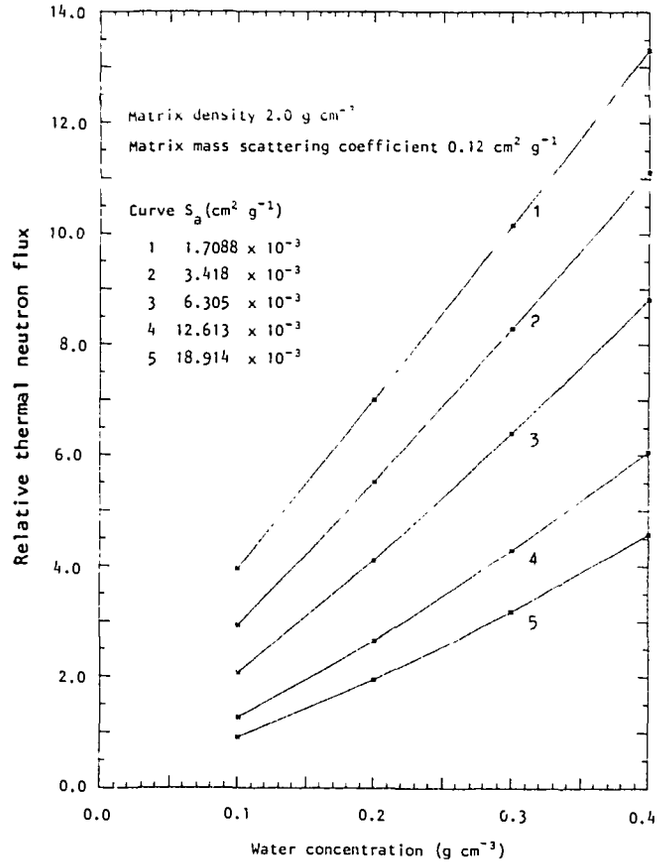

Figure 11 Detector response as a function of water content for various S_a: matrix density 2.0 g cm^{-3}

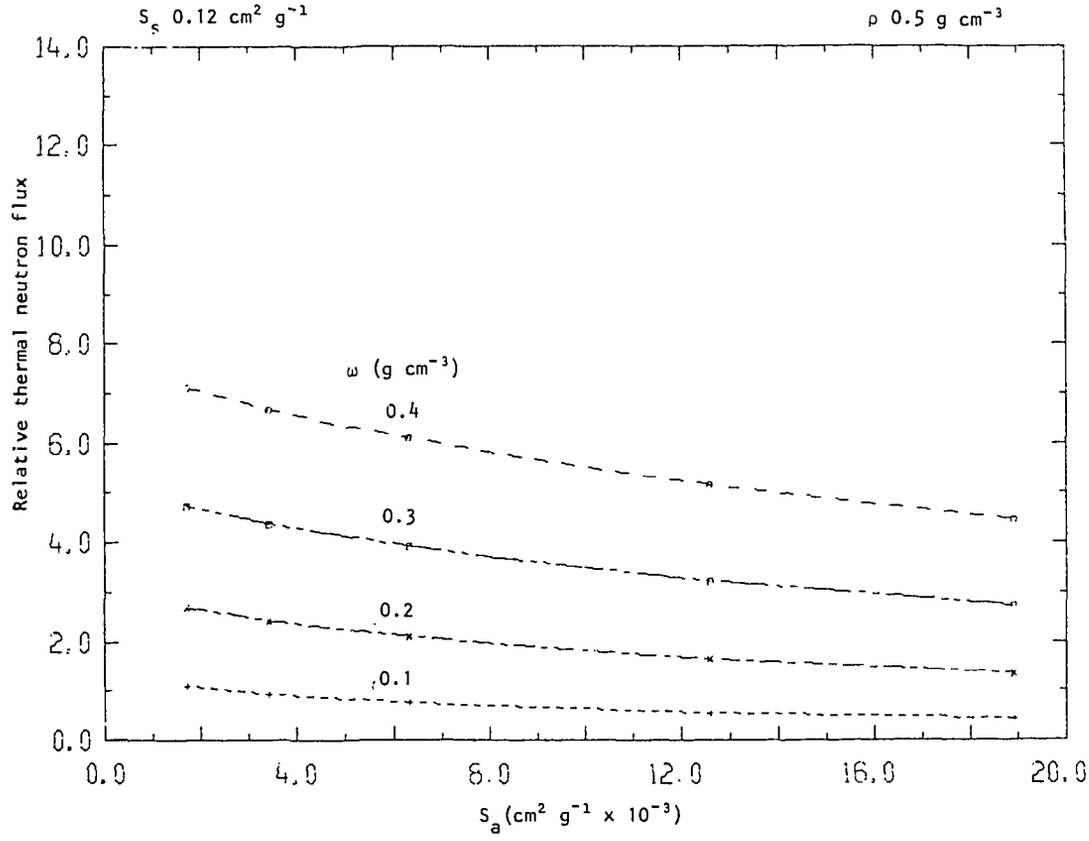

Figure 12 Detector response as a function of S_a for various water content; matrix density 0.5 g cm^{-3}

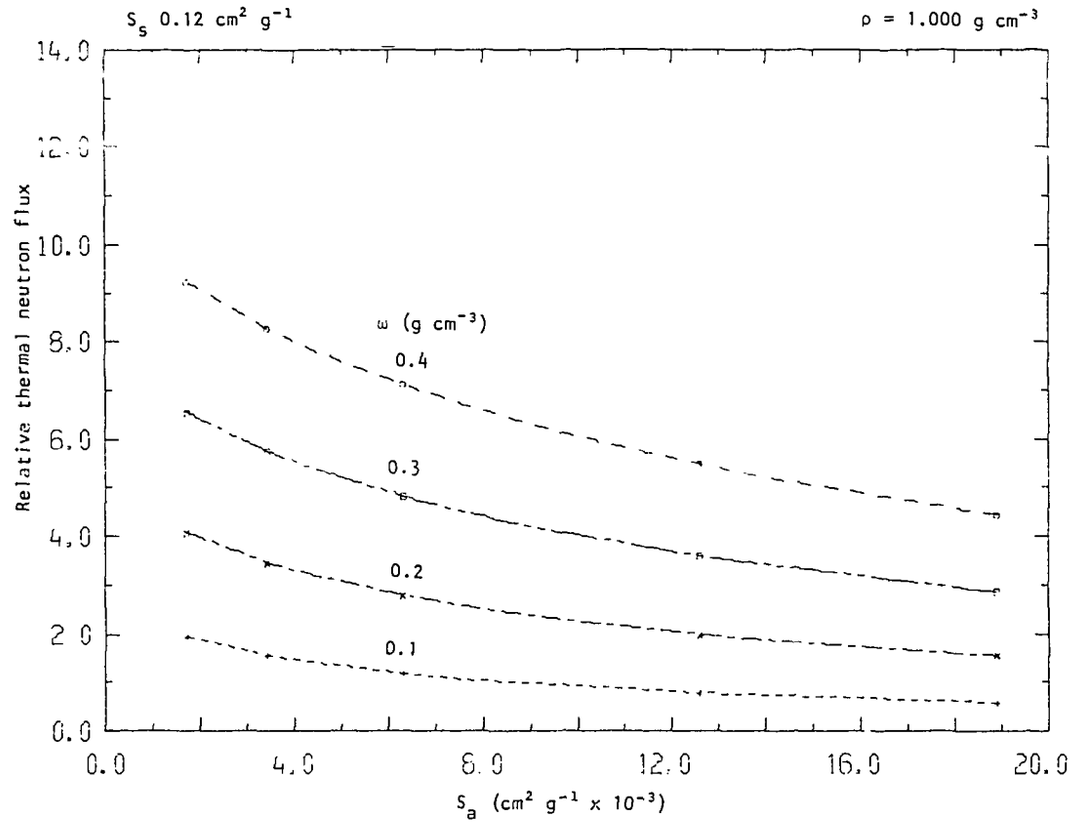

Figure 13 Detector response as a function of S_a for various water content; matrix density 1.0 g cm^{-3}

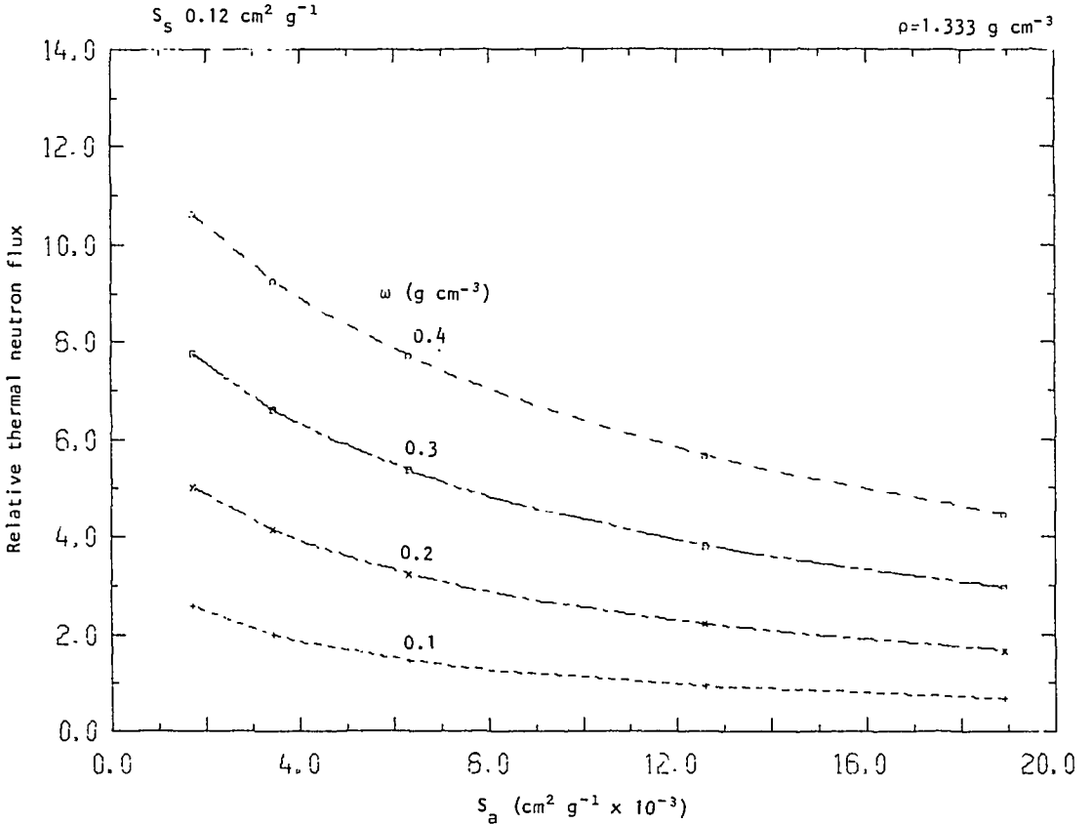

Figure 14 Detector response as a function of S_a for various water content; matrix density 1.333 g cm^{-3}

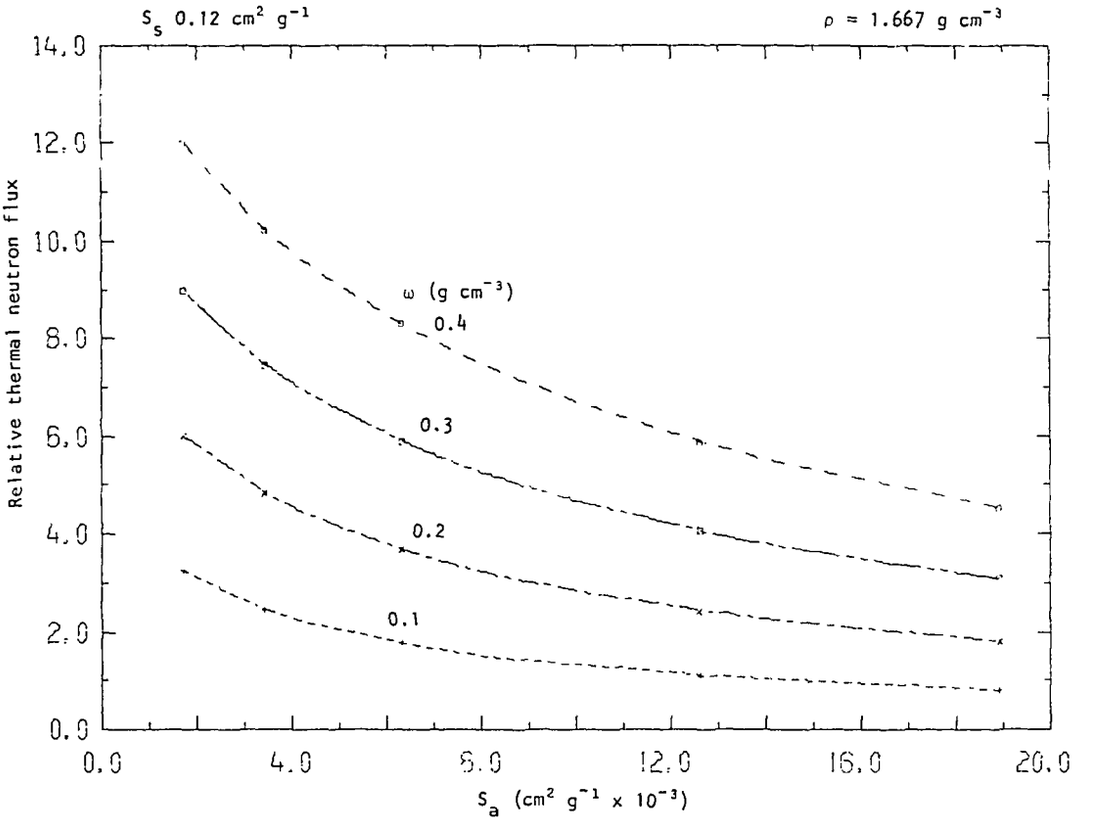

Figure 15 Detector response as a function of S_a for various water content; matrix density 1.667 g cm^{-3}

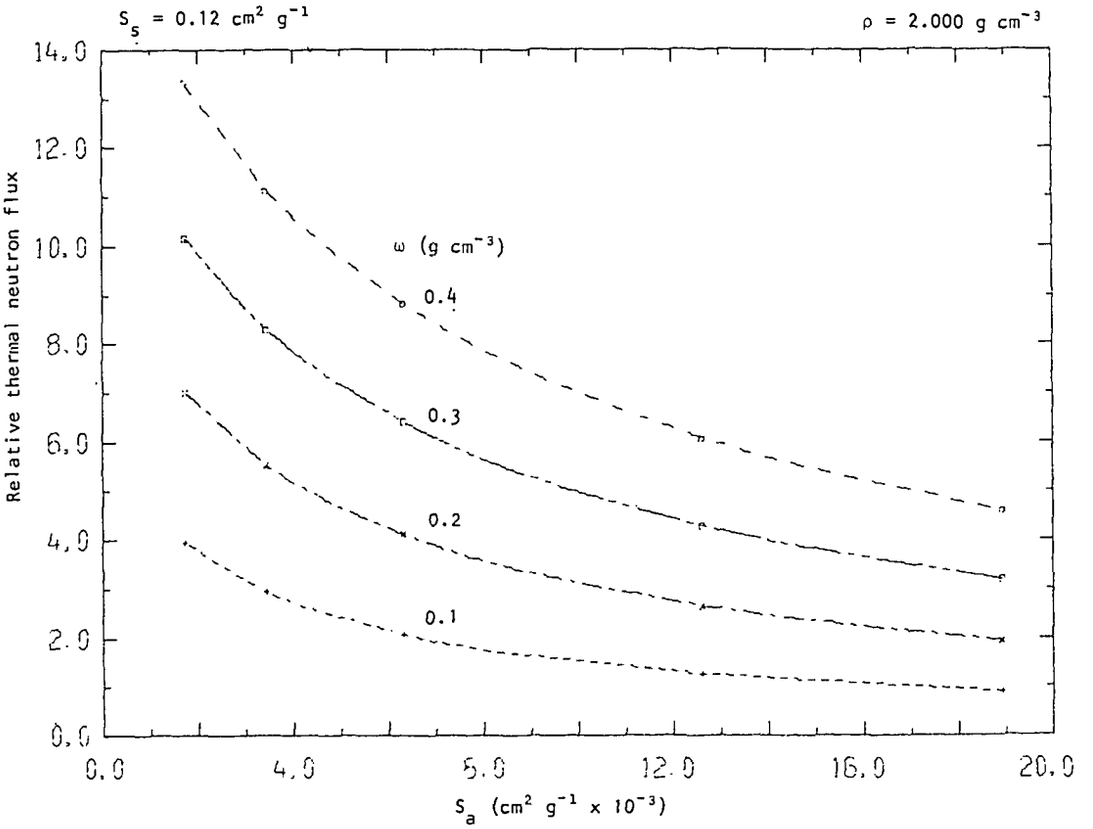

Figure 16 Detector response as a function of S_a for various water content; matrix density 2.0 g cm^{-3}

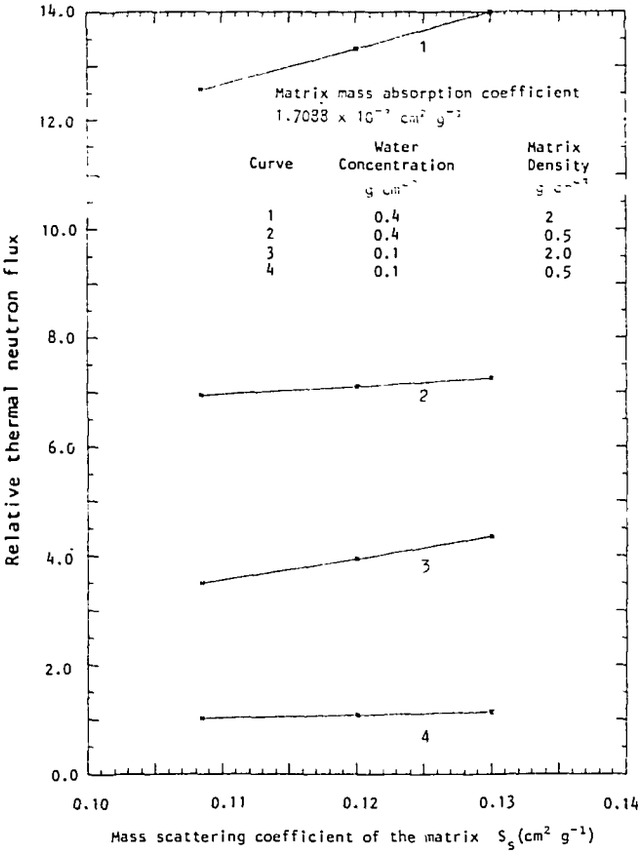

Figure 17 Detector response as a function of matrix mass scattering coefficient for various ω; S_a 1.71×10^{-3} cm^2 g^{-1}

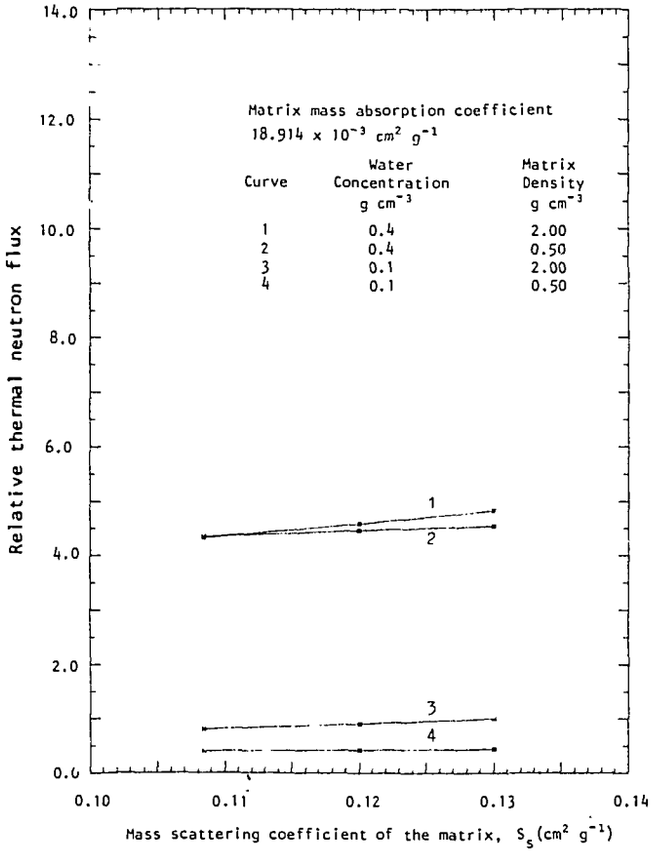

Figure 18 Detector response as a function of matrix mass scattering coefficient for various ω; S_a 18.91×10^{-3} cm^2 g^{-1}

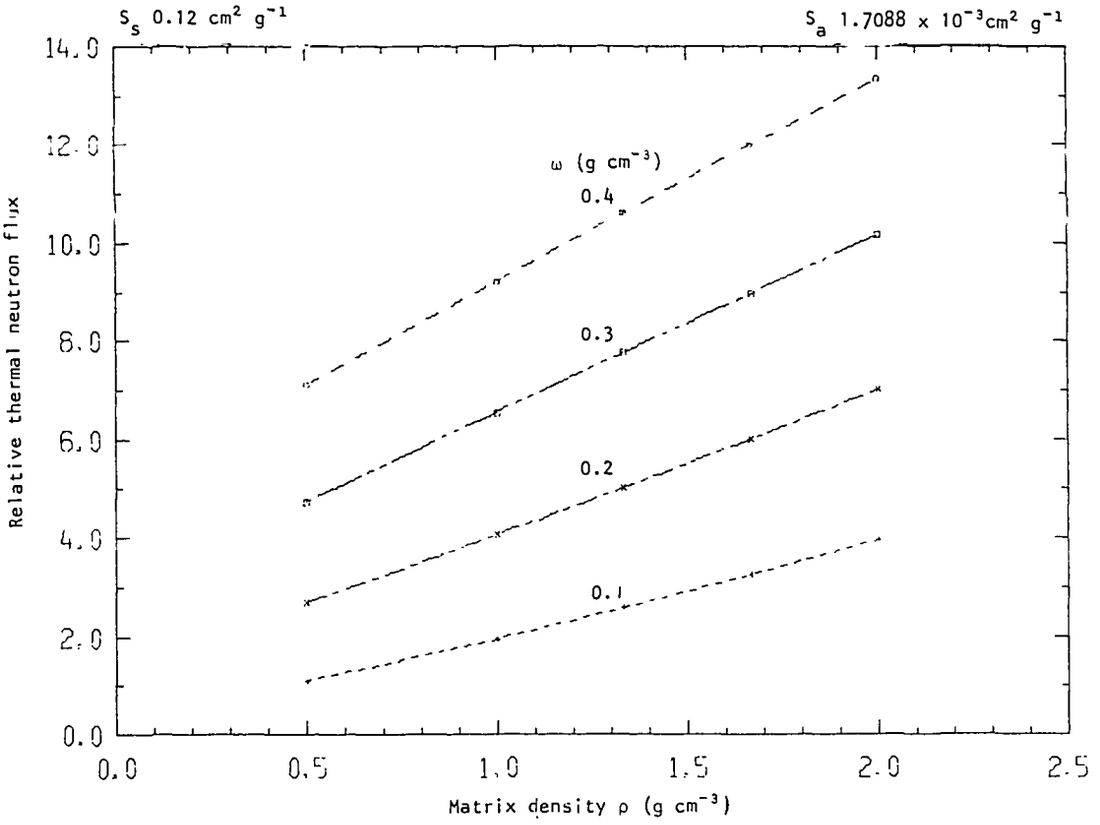

Figure 19 Detector response as a function of matrix density for various ω; S_a 1.71 × 10^{-3} cm^2 g^{-1}

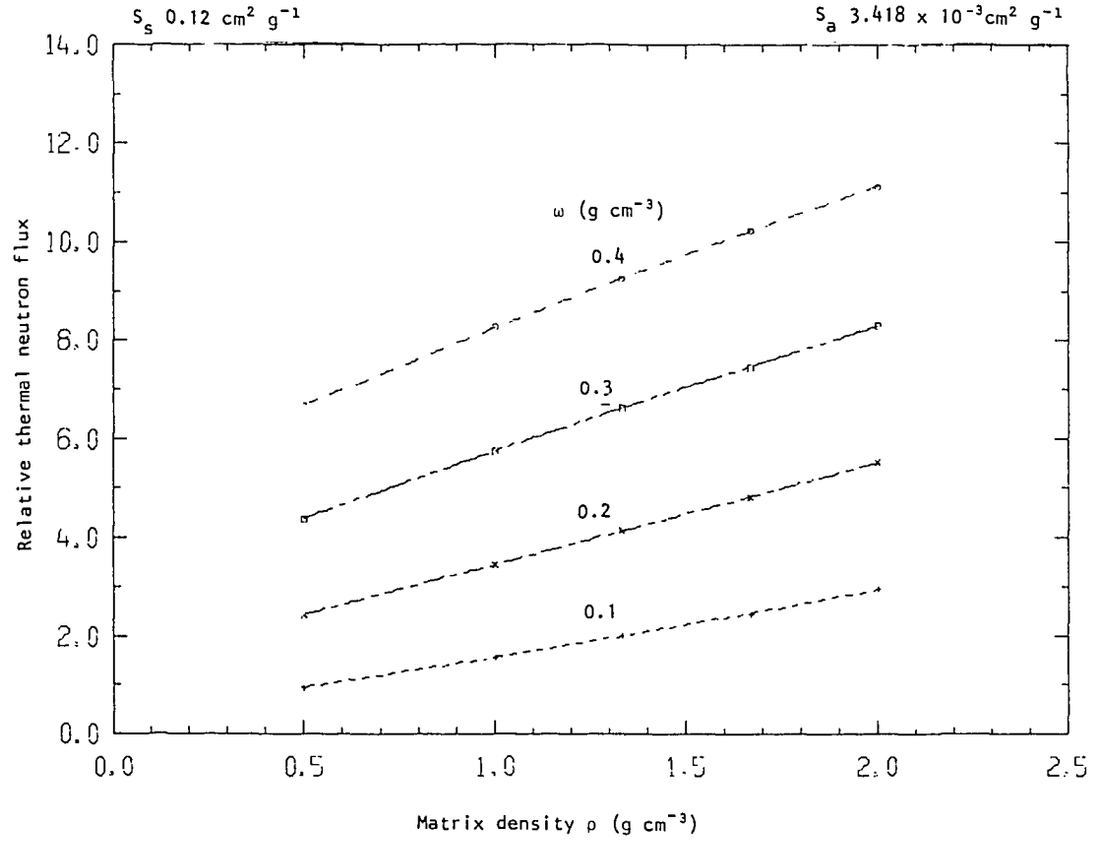

Figure 20 Detector response as a function of matrix density for various ω; S_a 3.42 × 10^{-3} cm^2 g^{-1}

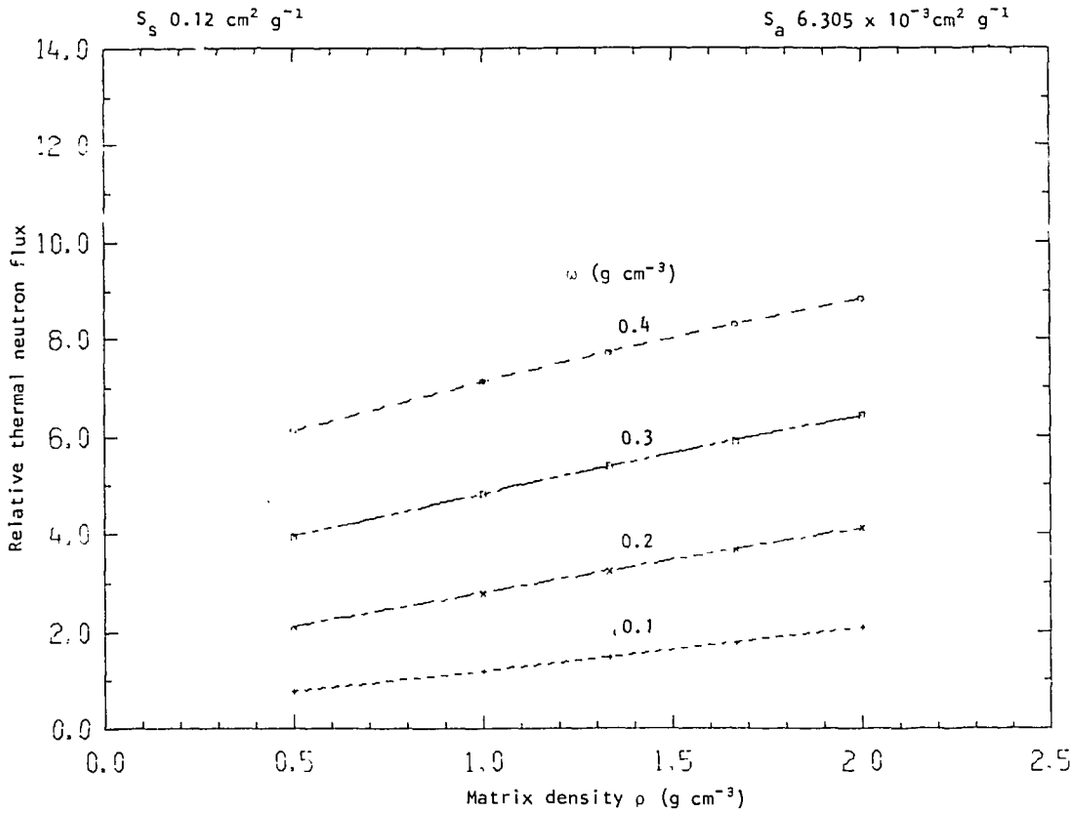

Figure 21 Detector response as a function of matrix density for various ω; S_a 6.31 $\times$ 10^{-3} cm^2 g^{-1}

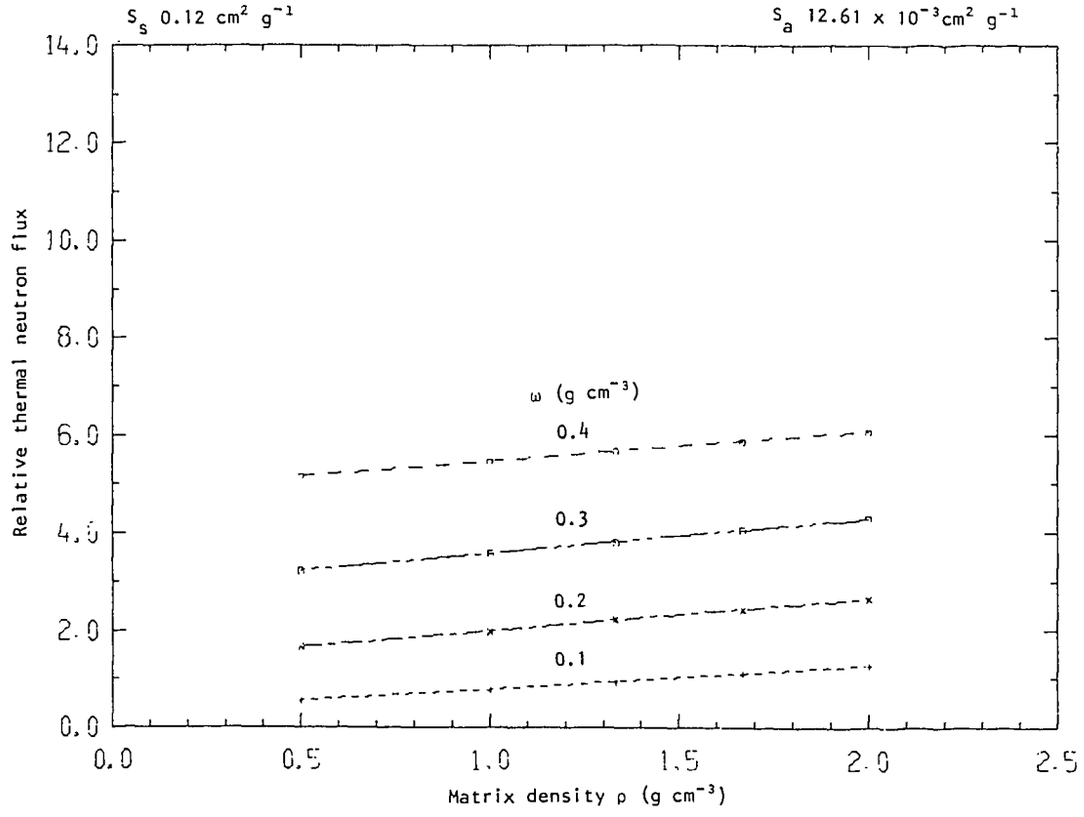

Figure 22 Detector response as a function of matrix density for various ω; S_a 12.61 $\times$ 10^{-3} cm^2 g^{-1}

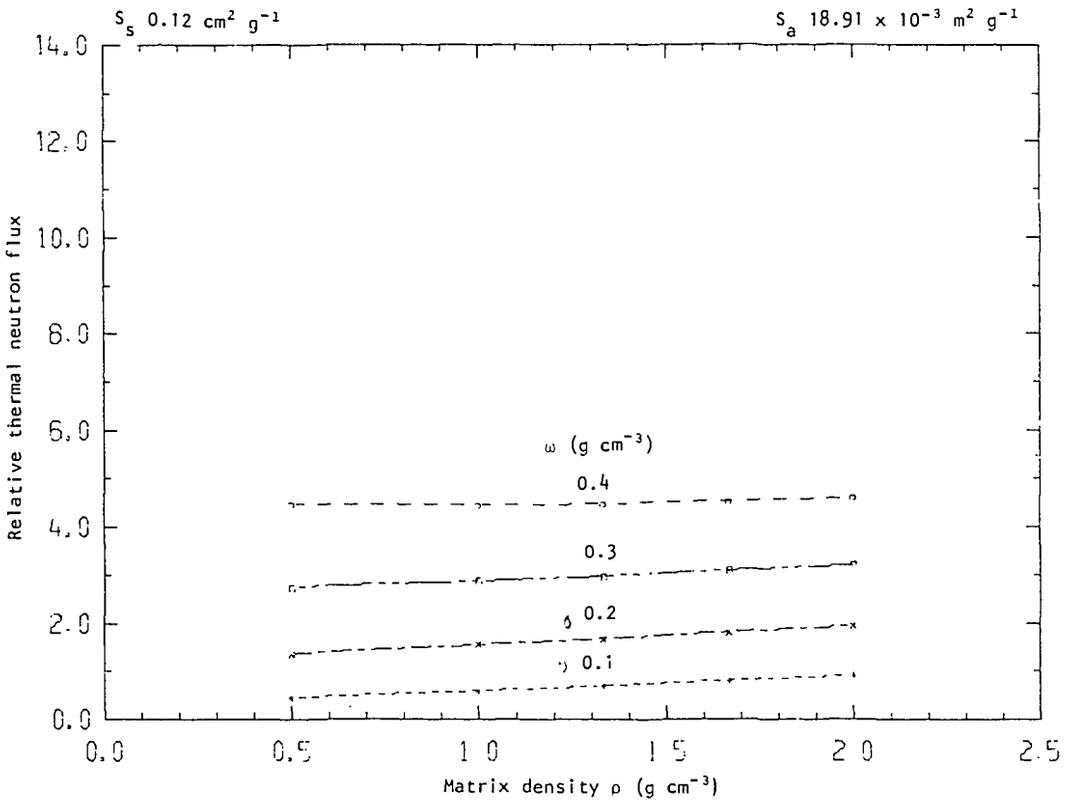

Figure 23 Detector response as a function of matrix density for various ω; S_a 18.91 $\times 10^{-3}$ cm^2 g^{-1}

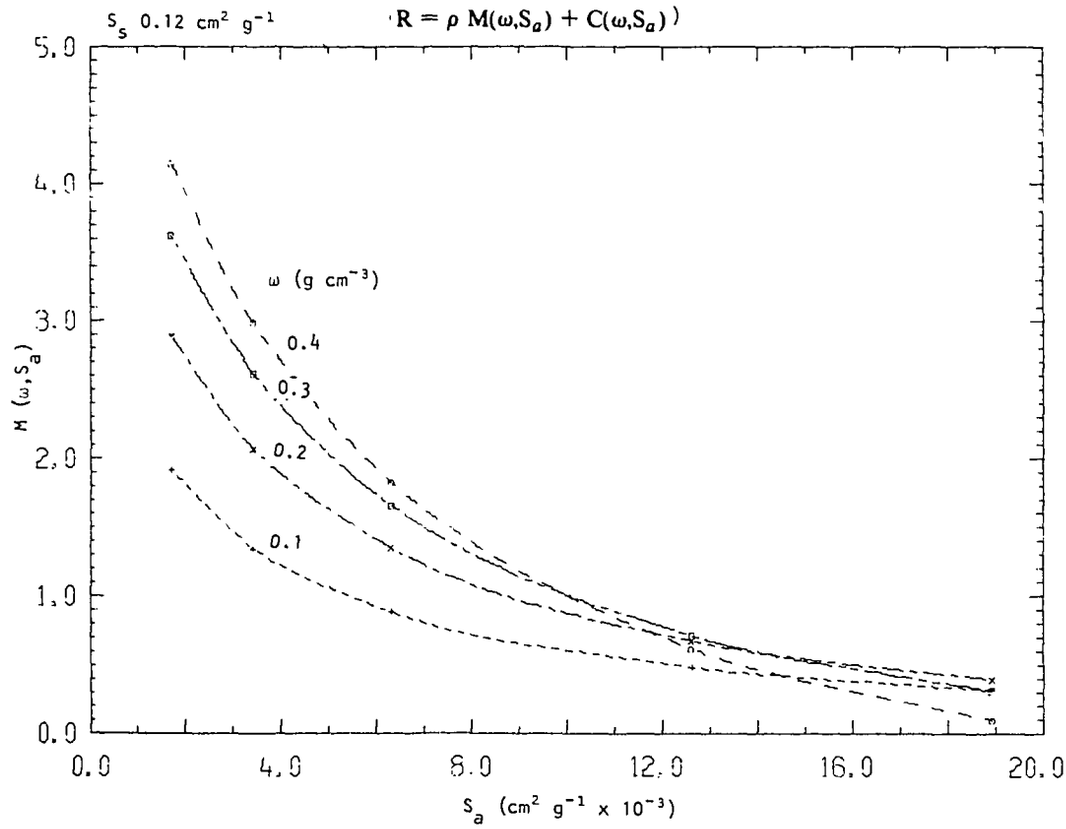

Figure 24a $M(\omega,S_a)$ as a function of S_a for various ω

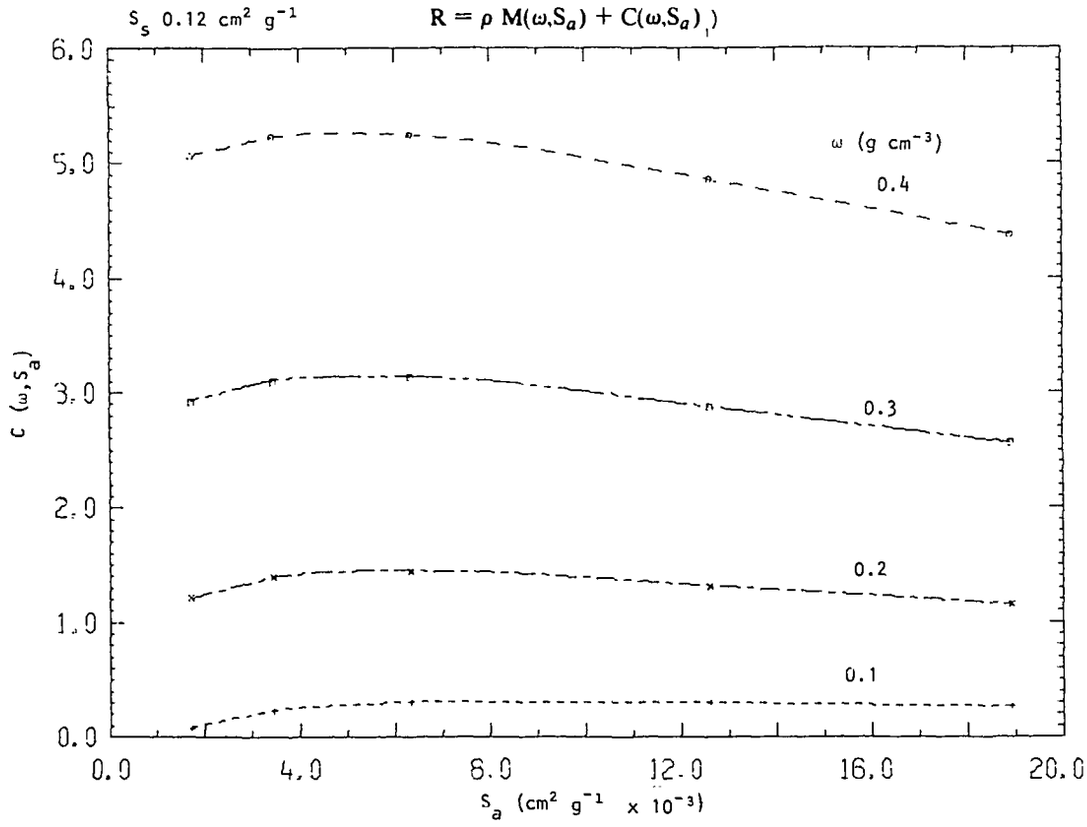

Figure 24b $C(\omega,S_a)$ as a function of S_a for various ω

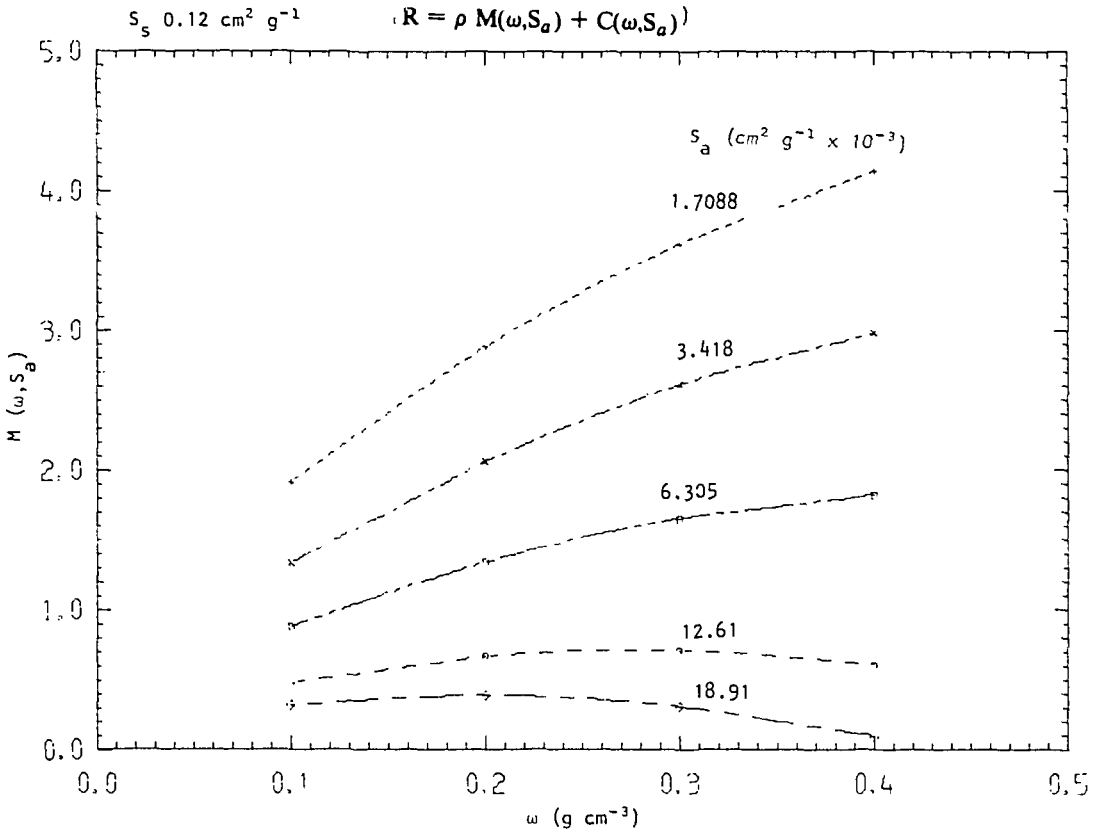

Figure 25a $M(\omega,S_a)$ as a function of ω for various S_a

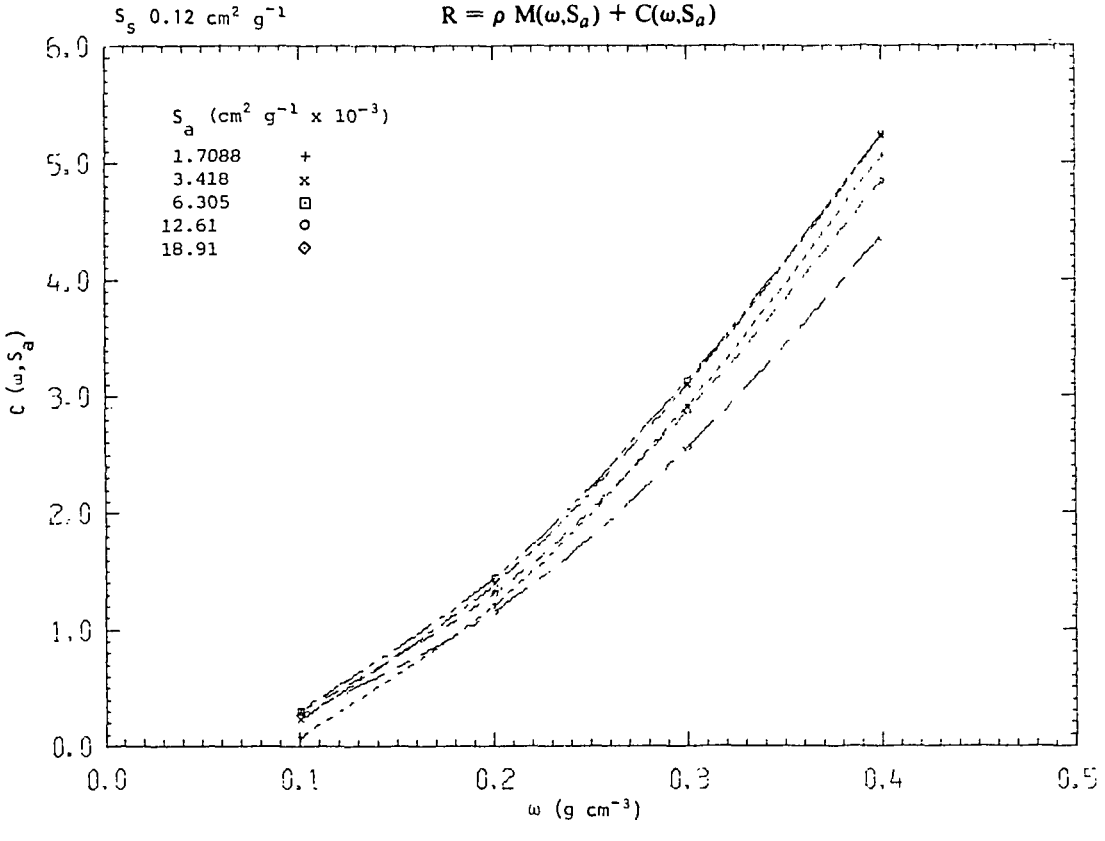

Figure 25b $C(\omega,S_a)$ as a function of ω for various S_a